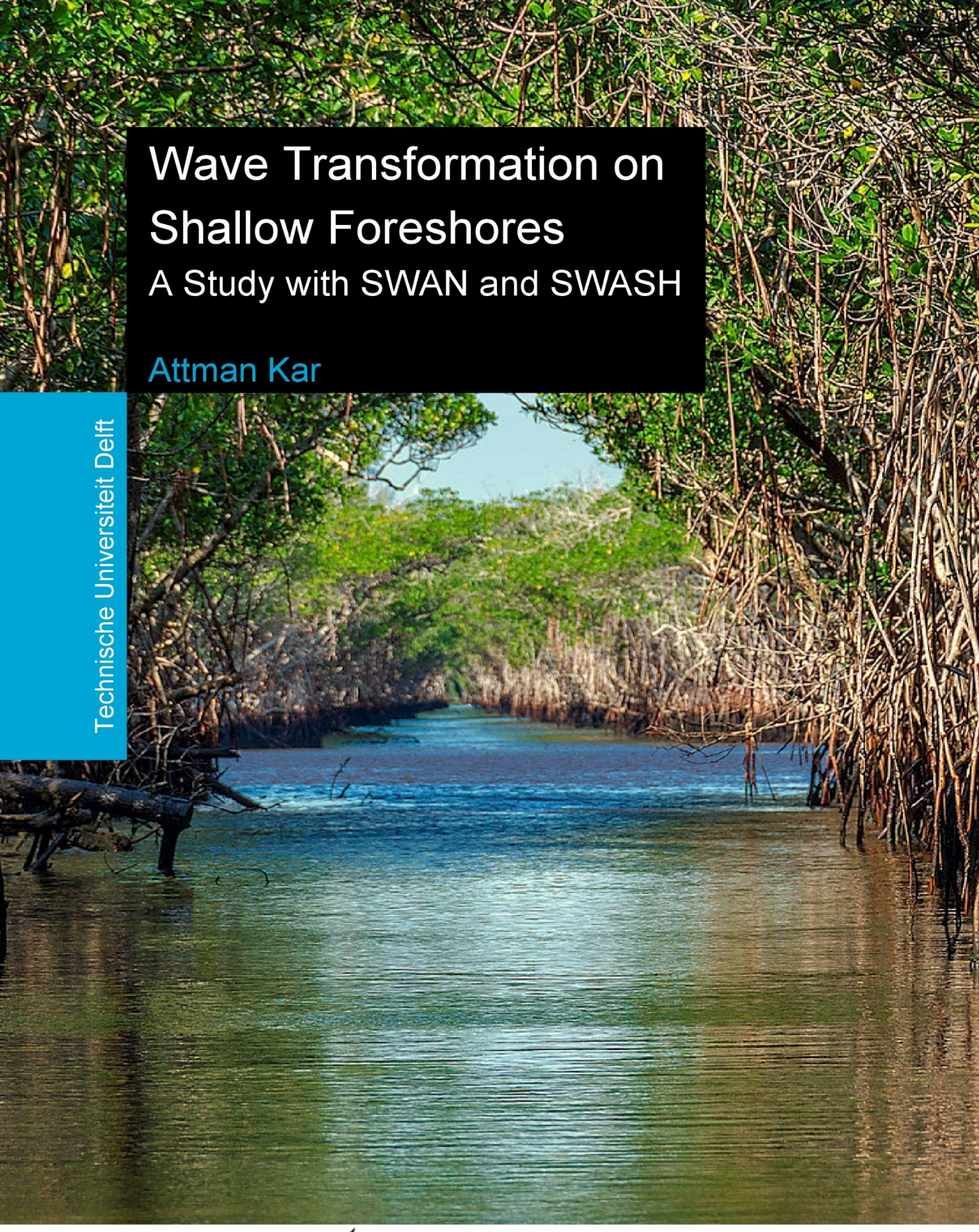

Wave Transformation on Shallow Foreshores

A Study with SWAN and SWASH

Attman Kar

Technische Universiteit Delft

Erasmus+ TU Delft Delft University of Technology CoMEM

Challenge the Future

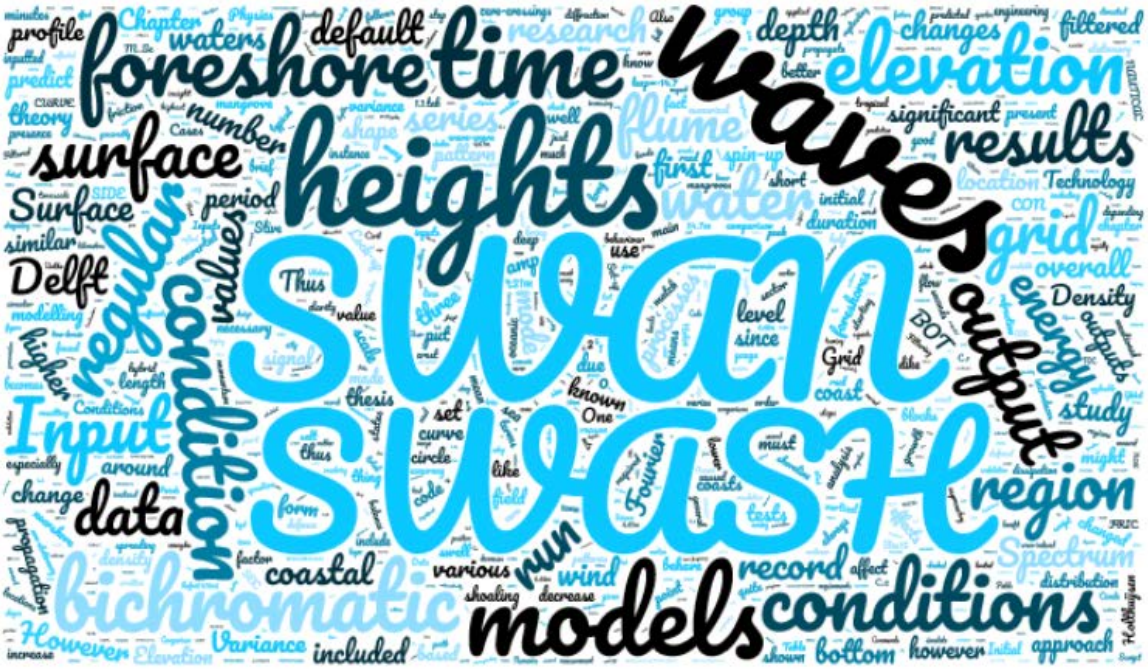

Keywords: CoMEM, SWAN, SWASH, wave, bichromatic wave, energy spectrum, wave transformations, shallow foreshores

Front Cover: A look through the mangrove forest in the Bhitarkanika National Park, located at the deltaic confluence of Brahmani and Baitarani rivers, in the state of Odisha, India.
(Adapted from the travel blog of grabon.in; Accessed 14 July 2017)

Word Cloud: www.wordclouds.com

WAVE TRANSFORMATION ON SHALLOW FORESHORES

A STUDY WITH SWAN AND SWASH

by

Attman KAR

in partial fulfilment of the requirements for the degree of

Master of Science

Civil Engineering

Coastal and Marine Engineering and Management (CoMEM)

at the Delft University of Technology, The Netherlands,
to be defended publicly on Thursday, 17 August 2017, at 14.00.

Thesis Assessment Committee:

Prof. dr. ir. S.G.J. Aarninkhof, Delft University of Technology, Chairman
Ir. H.J. Verhagen, Delft University of Technology
Dr. ir. M. Zijlema, Delft University of Technology
Ir. S.A.J. Tas, Ph.D., Delft University of Technology

An electronic version of this thesis is available at
http://repository.tudelft.nl/

Correspondence with the author may be directed to:
er.karattman@gmail.com

TU Delft

NTNU – Trondheim Norwegian University of Science and Technology
University of Southampton
UPC Universitat Politècnica de Catalunya BarcelonaTech
City University of London Est 1894

The Erasmus+: Erasmus Mundus MSc in Coastal and Marine Engineering and Management is an integrated programme including mobility organised by five European partner institutions, coordinated by the Norwegian University of Science and Technology (NTNU).

The joint study programme of 120 ECTS (European Credits) (two years full-time) has been completed by this student at the first three of the following five CoMEM partner institutions:

- Norges Teknisk-Naturvitenskapelige Universitet (NTNU) Trondheim, Norway
- Technische Universiteit (TU) Delft, The Netherlands
- University of Southampton, Southampton, United Kingdom
- Universitat Politècnica de Catalunya (UPC). BarcelonaTech. Barcelona, Spain
- City, University of London, London, United Kingdom

During the first three semesters of the programme, students study at two or three different universities depending on their track of study. In the fourth and final semester, an MSc thesis must be completed. The two-year CoMEM programme leads to multiple officially recognised MSc degree certificates. These will be issued by the universities that have been attended by the student. The transcripts issued with the MSc Degree Certificate of each university include grades/marks and credits for each subject.

Information regarding the CoMEM programme can be obtained from the programme coordinator:

Øivind A. Arntsen, Dr.ing.
Associate Professor of Marine Civil Engineering
Department of Civil and Transport Engineering
NTNU Norway
Telephone: +47-73594625 Cell: +47-92650455 Fax: +47-73597021
Email: oivind.arntsen@ntnu.no
URL: www.ntnu.edu/studies/mscomem

“ଜ୍ଞାନ ଆଲୋକିତ କରେ”

Knowledge Enlightens

SUMMARY

Across the world, the presence of humans in coastal regions is always increasing. Hydraulic forcing from extreme events is a large risk around the global coastlines, the risk being complicated by the increased human presence along the coasts.

The knowledge that vegetation can be used as a coastal protection measure is not something new. The benefits of vegetation have been seen throughout history and are being researched on till date. If we know to a certain confidence what the wave heights are at the shoreline, coastal defence structures, used as a hybrid protection measure, can be designed accordingly. Not much research has been done on the wave behaviour on shallow foreshores.

Localised studies have been previously done on tropical vegetated coasts, but there is a lack of efficient and accurate analysis on a large scale. As we bring more clarity on how waves transform and attenuate in a typically vegetated coast, some questions get answered, and some more questions arise, which also happened during the research done for this thesis.

Observed data, be it laboratory or field, is very crucial in validating numerical models. A laboratory experiment was done in the TU Delft Laboratory of Fluid Mechanics flume, for a complete vegetation-free profile, where the surface elevations were observed for different wavemaker input conditions.

A lot of numerical models have been developed that predict wave transformation and dissipation through vegetated foreshores. However, these models lack validation from observed data. This thesis first focuses on understanding the wave transformation for two unique (and mainly theoretical) wave conditions: a regular sinusoidal wave and a bichromatic wave. It was checked if the transformation is reflected in the models – SWAN and SWASH, which they did.

The research proceeded on to validating the models by comparing the wave heights observed in the laboratory experiment versus when the models were inputted with the same conditions, including inputting the observed data into the models. When the laboratory conditions were replicated, the SWASH results obtained correlated quite well with what was observed in the laboratory. The same was not true in the case of SWAN.

When a spectral analysis was done for the observed data, a presence of very low frequencies (VLF) as well as some minor higher frequencies was noticed. To check its effect, if any, on the model results, they were filtered out. Both the original and filtered data was inputted into the models. The difference in the foreshore region was more distinct in the filtered case, i.e., making a bichromatic elevation input purer resulted in more pronounced undulations in the wave heights than what was predicted in the unfiltered data. This result does not fit well with the existing knowledge on wave dissipation processes. It is widely known that the presence of VLFs and higher frequencies are the driving mechanisms that result in the undulations in the foreshore region, but the predicted results were exactly opposite to this knowledge.

What can be thought of from the anomaly is that the presence of various frequencies (that is, waves with different periods) counteract each other's effects and make the undulating wave heights milder, but when the signal is made purely bichromatic, it leads to more distinct undulations. This proposition is also backed by the similar SWASH results for the laboratory condition-replicating theoretical inputs. This anomaly needs further investigation.

Another interesting observation was that the changes happening in the offshore region did not affect the results in the foreshore region, for varying parameters in SWAN.

SWASH can be concluded as a better model for predicting wave heights, especially in the foreshore region. SWAN could not predict the fluctuations in the wave heights. Obtaining the wave heights at the shoreline with SWAN, and designing a dike with those results, for example, will lead to disastrous consequences, as SWAN underestimates the wave heights.

The study is limited by the consideration of hydrodynamics only, and by the many simplifications made to simulate the conditions. One of the recommendations formulated is to obtain field data and to make a similar comparison with the models to corroborate (or correct) the observations made.

This study tried to see the correlation between the models and observed data in the laboratory, for simple (and somewhat purely theoretical) cases. It is, nonetheless, a starting point for more complicated cases, the basis for which can be laid on this study.

SAMENVATTING

Verspreidt over de wereld groeit de bevolking in de kustgebieden. In deze kustgebieden vormt de aanwezigheid van water in toenemende mate een risico, wat versterkt wordt door de bevolkingsgroei in deze gebieden.

De kennis om begroeiing toe te passen als maatregel voor kustbescherming is geen nieuw feit. Tot op heden wordt er nog steeds onderzoek gedaan naar vegetatie mogelijkheden. Indien met een zeker betrouwbaarheidsinterval gesteld kan worden wat de golfhoogte is op een bepaalde positie, dan kunnen kustbeschermingsvoorzieningen getroffen worden als hybride beschermingsmaatregel. Tot op heden is er niet veel onderzoek gedaan naar golfimpact op licht hellende ondiepe kustwatergebieden.

In het verleden zijn er enkele lokale onderzoeken uitgevoerd voor kustgebieden in tropisch gebied maar er is een gebrek aan effectief en nauwkeurige analyses op grote schaal. Zodra er meer bekendheid komt omtrent de transformatie van golven in een standaard begroeid kustgebied worden er enkele antwoorden opgehelderd en tegelijkertijd komen er nieuwe vragen op, zo ook tijdens het onderzoek dat gedaan is in deze thesis.

Data van zowel testopstellingen alsmede als in de praktijk zijn van groot belang voor de validatie van numerieke modellen. In de TU Delft Laboratory of Fluid Mechanics stroomgoot is een experiment uitgevoerd voor een onbegroeid profiel waar de oploop zijn waargenomen voor verschillende golfcondities.

Veel numerieke modellen zijn ontwikkeld met als doel een voorspelling te doen omtrent golf transformatie en breking voor begroeide kustwatergebieden. Helaas missen deze modellen de validatieslag met behulp van gemeten data. De focus van deze thesis is primair op het begrijpen van golftransformaties voor twee unieke golfcondities: een reguliere sinusvormige golf en een bi-chromatische golf. Er is onderzocht in hoeverre de transformatie is gereflecteerd in de numerieke modellen SWAN en SWASH.

Het onderzoek vervolgde met de validatie door middel van het vergelijken van de golfhoogtes die voortkomen uit experimenten en de numerieke modellen. Op het moment dat de experimenten onder dezelfde condities werden herhaald, bleek dat de SWASH-resultaten een hoge correlatie hadden met de geobserveerde resultaten van de experimenten. Dit gold echter niet voor de SWAN-resultaten.

Tijdens het uitvoeren van een spectraalanalyse bleek uit de data dat er zeer lage frequenties (VLF) en enkele hoge frequenties in het signaal zaten. Om te voorkomen dat deze frequenties eventueel impact hebben op de model resultaten, zijn deze eruit gefilterd. Zowel de originele alsmede de gefilterde resultaten zijn toegepast in de numerieke modellen. Dit resulteerde in een verschil in kustwaterregio, wat betekent dat een meer puur bi-chromatische golf resulteert in meer golvingen in de golfhoogte dan dat vooraf was voorspeld op basis van de ongefilterde data. Dit strookt niet met de huidige kennis over golfdissipatie processen. Het is bekend dat VLF's en HF's de drijvende kracht zijn in golvingen in het kustwatergebied, iets wat tegenstrijdig is met de gevonden resultaten.

Wat geconcludeerd kan worden op basis van de verwachting is dat de aanwezige frequenties (ook wel golven met verschillende periodes) elkaar uitdoven wat resulteert in verminderde golvingen; iets dat niet volgt in geval van puur bi-chromatische signalen. Dit resultaat volgt eveneens uit de SWASH-resultaten van de testen die laboratorium gevallen repliceren. Voor deze tegenstrijdigheid zou nader onderzoek gedaan moeten worden.

Een ander interessante waarneming waren de veranderingen in het offshore gebied voor verschillende parameters in het SWAN-model. Deze hadden geen effect op het kustwatergebied.

Het kan geconcludeerd worden dat het SWASH-model betere uitkomsten geeft voor met name het kustwatergebied. SWAN kon de schommelingen in de golfhoogte niet voorspellen. Indien SWAN gebruikt wordt voor het ontwerpen van dijken, kunnen de gevolgen rampzalig zijn vanwege de onderschatting van de golfhoogte.

Dit onderzoek is beperkt tot alleen hydrodynamische aspecten, en door de vele versimpelingen om de simulaties uit te vormen. Een van de aanbevelingen is om velddata te verwerven voor het kalibreren van de modellen met de nu verkregen observaties.

In dit onderzoek is getracht om de correlatie te vinden tussen de modellen en de laboratorium data onder versimpelde omstandigheden. Het is desondanks een startpunt voor de meer geavanceerde onderzoeken.

SAMMENDRAG

Over hele verden er tilstedeværelse av mennesker i kystområder er stadig økende. Hydrauliske krefter fra ekstreme hendelser er en stor risiko langs verdens kystlinjer, en risiko som kompliseres av økende menneskelig nærvær langs kystene.

Kunnskapen om at vegetasjon kan bli brukt som en beskyttelse ved kysten er ikke nytt. Fordelene vegetasjonen bringer med seg er noe som har blitt sett igjennom historien og forskes på den dag i dag. Dersom vi med en viss sikkerhet kjenner bølgehøyden langs kystlinjen, kystforsvarsstrukturer brukt som en hybrid, sett i forhold til beskyttelse, kan bli utformet slik. Lite forskning har blitt gjort på bølgers adferd i gruntvannsområder nær kysten.

Lokaliserte studier har tidligere blitt gjennomført i tropisk vegeterte kyster, men det er mangel på nøyaktige analyser på større skala. Når vi får mer klarhet om hvordan bølger oppfører seg i tropisk vegetert kyst, gir det svar på noen spørsmål mens andre spørsmål oppstår, noe som også skjedde i forbindelse med forskningen til denne oppgaven.

Observerte data, det være seg laboratorium eller fra felt, er svært viktig for å validere numeriske modeller. Et laboratorieforsøk utført ved TU Delft Laboratory of Fluid Mechanics, for en fullstendig vegetasjonsfri profil, hvor overflatehøyden ble observert for ulike bølger med ulike inngangsbetingelser.

Mange numeriske modeller har blitt utviklet og for å kunne forutse bølgetransformasjon og spredning gjennom vegeterte gruntvannsområder nær kysten, men disse modellene mangler bekreftelse fra observerte data. Denne oppgaven fokuserer først på å forstå bølgetransformasjon for to unike (og hovedsakelig teoretiske) bølgebetingelser: en vanlig sinusformet bølge og en dikromatisk bølge. Det ble undersøkt om transformasjonen er reflektert i kandidatens modeller - SWAN og SWASH, noe de gjorde.

Videre ble forsøk utført for å validere modellene ved å sammenligne bølgehøyder observert i laboratorieforsøket mot når modellene ble innputtet samme forhold, inkludert inputting av observert data i modellene. Når laboratoriebetingelsene ble replikert, oppnådde SWASH-resultatene ganske god korrelasjon med det som ble observert i laboratoriet. Det samme var ikke tilfelle for SWAN.

Når spektralanalysen ble utfor for de observerte dataene, ble det observert en tilstedeværelse av veldig lav frekvens (VLF) så vel som noen høye frekvenser. Filteret ble benyttet for å utforske hvilke effekter, om noen, disse frekvensene har. Både de opprinnelige og de filtrerte dataene ble brukt i modellene. Forskjellene i gruntvannsområdene var mer tydelig i det filtrerte tilfellet, resulterte i mer en tydeligere bølgehøydeform enn der som var i de ufiltrerte dataene. Dette passer ikke godt med eksisterende kunnskap om bølgedissipasjonsprosesser. Det er allmennlære at VLFer og høyere frekvenser er drivmekanismen som resulterer i bølgeformen i gruntvannsområdene, men de forventede resultatene var helt motsatt til denne kunnskapen.

Det man kan lære fra anomalien er at forskjellige frekvenser (nemlig bølger med ulike perioder) motvirker hverandres effekter og gjør bølgehøyder mildere, men når signalet blir gjort helt dikromatisk, fører det til mer tydelige svingninger. Dette påstanden støttes også av lignende SWASH-resultater for laboratoriebetingelser-replikere teoretiske inputs. Denne anomalien trenger definitivt ytterligere undersøkelser.

En annen interessant observasjon er at endringene i offshore-områder, for varierende parametere i SWAN ikke påvirket resultatene i gruntvannsområder.

En kan konkludere med at SWASH er en bedre modell for å forutsi bølgehøyder, spesielt i gruntvannsområder. SWAN kan ikke forutsi svingningene i bølgehøyder. Å oppnå bølgehøyder ved kystlinjen med SWAN, og designe et dike med disse resultatene, vil for eksempel føre til katastrofale konsekvenser, da SWAN undervurderer bølgehøyder.

Studien er begrenset av hensynet til hydrodynamikk og av de mange forenklingene som er gjort for å simulere forholdene. En av anbefalingene er å skaffe feltdata og å gjøre en lignende sammenligning med modellene for å bekrefte (eller korrigere) observasjonene.

Denne studien forsøkte å finne sammenheng mellom modellene og observerte data fra laboratoriet, for enkle (og rent teoretiske) tilfeller. Det er likevel bare et utgangspunkt for mer kompliserte caser, hvor denne studien kan fungere som et grunnlag.

PREFACE

Writing briefly takes far more time than writing at length.
Carl Friedrich Gauss

This M.Sc. thesis draws curtains on my studies of the European Commission funded Erasmus+ Masters in Coastal and Marine Engineering and Management (CoMEM). I completed CoMEM by studying at three leading research universities in Europe in the field of Coastal Engineering: *Norwegian University of Science and Technology*, Norway, *Delft University of Technology*, The Netherlands, and *University of Southampton*, United Kingdom. The research for this thesis was done at the Delft University of Technology.

A little more than two years ago, when I was a fresh Bachelor near-graduate in Civil Engineering, I got my admission letter to join the M.Sc. CoMEM programme. I was ecstatic, to say the least. Little did I know then how exciting these two years were going to be and what was in store for me. The past six months spent working on this thesis and the last two years of this program have flown past. It has been a challenging but eventually an enriching experience. I consider myself extremely lucky to have been given this chance to study in Europe, to meet a lot of new people, and to work in a discipline which has always been fascinating to me, since childhood. These last two years have forced me to grow and mature as a human being so much that it is incomprehensible. I have gained and equally lost so much.

I would first like to thank my thesis supervisory committee, without whose support I could not have completed my thesis. Ir. Henk Jan Verhagen, thank you very much for taking me as your student, despite your busy schedule. I found it really rewarding to work with you, especially on a topic which always fascinated me. Thank you for providing me with inspiration when I lacked it and for guiding me when I needed it. I always enjoyed and learnt a lot from our discussions, academics and beyond. To Dr. Stefan Aarninkhof, thank you for chairing the committee, keeping me on track, and always asking insightful questions. Your valuable comments during the progress meetings helped me to shape my thesis in an efficient manner. To Dr. Marcel Zijlema, thank you very much for answering my questions and keeping me on the right path, so I do not make mistakes with the models. I might have bored you a lot with sometimes silly questions, sorry for that. To Ir. Silke Tas, you have been much support during these months. Thank you for answering questions and for our academic and non-academic discussions.

I thank the European Commission and the CoMEM board to provide me with this chance of participating in this M.Sc. programme. *Tusen takk*, Sonja Hammer and Øivind Arntsen, for organising the programme and always answering questions on logistical arrangements as they arose. To Arne Aalberg, thank you very much for giving me the out-of-the-world opportunity of studying at UNIS, Svalbard, last summer. I cannot ever forget the experience of sighting polar bears in their native environment.

Several other people have been instrumental, directly or indirectly, in the formation of this thesis. To my fellow CoMEM classmates – Alba, Arefin, Belen, Bruna, Encarna, Ermano, Hithaishi, Imran, Krasi, Laura, Renan, Sanduni, and Xabi – thank you for all the

cherished memories. We faced everything together, inside and outside classes, and overcame everything with flying colours.

Thank you very much, Jochem Dekkers and Dr. Marion Tissier, for sharing the laboratory data from your research project, on which the chapter on model validation is based. To my officemates at TU Delft: Bart, Marloes, and Sanduni, thank you for our lunches and coffee breaks together, and Bart – for your constructive comments throughout this research. To my cousin, Pooja – thank you for always inspiring me to achieve more and more in life, as well as inspiring me on how to compose this thesis.

To the CoMEM organisers at TU Delft: Bas Hofland, Madelon, Marieke, and Qing-yi, thank you very much for all the clarifying answers and organising different things around. Inge and Otti, thank you for bearing with me while making different administrative arrangements for me.

Heartfelt thanks go out to my friends, even if I cannot mention them all here. Vikramjeet, you have been a pillar of support throughout these years. Thank you very much for all the Skype and WhatsApp calls and chats. Grethe – *Tusen takk for all støtte gjennom årene*. *Jeg kan ikke takke deg nok.* To Bipul, César, Sigurd and family, and Tatha, thank you for all the time we spent together in Norway. To Alex, Emma, Joris, Megan, and Will, thanks for a great time in Southampton. To Carl and Nader, thank you very much for making my research period bearable by making me learn about your countries and answering all sorts of questions on your homelands.

My Dutch friends, with special mentions for Leonie, Marijke, Regina, and Vincent – thank you very much for making me feel at home in The Netherlands, helping me in all sorts of things, whenever I needed it the most. To Martin and Bjarte - *Takk for at du holder min norske ånd i live, og for oversettelsen av sammendraget til norsk (bokmål).*

Arno, onze vriendschap is een van de beste dingen die mij in mijn tijd in Nederland is overkomen. Ik kan je niet genoeg bedanken voor de goede band die wij hebben gekregen; je antwoorden op mijn vragen over de Nederlandse taal en cultuur tijdens onze eindeloze discussies en over zo veel meer dingen gedurende onze lange koffiepauzes en lunches. Bedankt dat jij er was in zowel goede als slechte tijden. Daarnaast mijn dank voor het vertalen van de samenvatting in het Nederlands.

Last but most importantly, I am deeply grateful to my mother, Tanima, and father, Soubhagya, for making me who I am today. You both always supported me unwaveringly, my aspirations, and my decision to go abroad and follow my curiosity. To my dear sister, Aditi – thank you very much for always being there for me. Thank you for your everlasting love and support.

ଧନ୍ୟବାଦ | Thanks | Bedankt | Takk | Dankie | Gracias | Obrigado | धन्यवाद | ಚಿತ್ತಾಯಿ | با تشکر

Attman Kar
Delft, August 2017

CONTENTS

LIST OF FIGURES

NOMENCLATURE

List of Symbols

Symbol	Units	Description
a	m	Wave amplitude
d	m	Water depth
E	m^2/Hz	Energy
f	Hz	Frequency
f_p	Hz	Peak frequency
g	m/s^2	Acceleration due to gravity
H	m	Wave height
H_{rms}	m	Root mean square wave height
H_s	m	Significant wave height
k	m^{-1}	Wave number (2π/L)
L	m	Local wavelength
m_0	m^2	Zeroth-order moment (area)
t	s	Time
T	s	Wave period
T_p	s	Peak wave period
x	m	Coordinate perpendicular to shoreline
z	m	Bottom level
η	m	Surface elevation, Water level set-up
ω	s^{-1}	Angular frequency (2π/T)
σ_η	m	Standard deviation
θ	°	Mean wave propagation direction
θ_{peak}	°	Peak wave propagation direction

List of Abbreviations

Abbreviation	Description
GUI	Graphical User Interface
JONSWAP	Joint North Sea Wave Project
NOAA	National Oceanic and Atmospheric Administration
SWAN	Simulating Waves Nearshore
SWASH	Simulating Waves till Shore
UNEP	United Nations Environment Programme
VDS	Variance Density Spectrum
VLF	Very Low Frequency

1

INTRODUCTION

You never really understand an issue or know how to help
resolve it until you involve yourself in the issue.
Then you begin to understand it,
to identify the principal parties, and actors involved,
and begin to realise how to change it.
Paulo Freire

This chapter introduces the reader to the general problem that this thesis study tries to bring clarity on, with the background and motivation, along with giving an outline of how this thesis is described.

1.1. Background

Humans live on a planet whose 71% of the surface is covered by water, be it oceans, seas, rivers or lakes. The early civilisations started and grew along the coasts and river banks. In today's world, if we want to build a new city, for instance, the factor that most affects the location of this new city, more than anything else, is water. Oceans have always been and still are what connects the world. There is no other means of transport that can move such an enormous amount of cargo for so little. Moreover, by extension again, if the new city is located far from the coast, it will still cost to bring the cargo over land. This is also a factor why the geographically efficiently placed towns (such as a coastal city) proliferate over centuries (or even on a decadal scale). Today, approximately half of the world's population live within 60 kilometres of a coastline (UNEP, 2017). Small & Nicholls (2003) also identified that within the 100-kilometre region from the coast, the population density is almost three times the average population density of the planet. As the coastal cities grow, so as the consequences of damages, social and economic, in the case of a disaster. Due to this rapid increase in population and infrastructure, tropical coastlines are under high pressure. The protection of coastal communities becomes even more important with the growth in population within the coastal zone (Small & Nicholls, 2003).

Mangroves are woody trees of several taxonomic groups. Using satellite imagery and image classifications, Giri et al. (2011) determined the total mangrove cover in the year 2000 to be 137,760 km^2, spread among 118 countries. They are mostly found on tropical or low-latitude coasts (Figure 1.1), in the inter-tidal regions, and form a highly productive ecosystem. At the same time, they provide the necessary protection against extreme events and accumulate sediment to prevent coastal erosion (Bosboom & Stive, 2015). Therefore, they help in developing coastal communities' resilience by minimising the damage caused by extreme events.

Figure 1.1: Global distribution of mangrove forests (Giri et al., 2011)

The fact that vegetation helps in wave attenuation is getting wider acknowledgement. Many coastal protection schemes have come up in the past few years. The goal is to enhance the role of flora in the protection and reduce the intervention by humans, depending on the actual situation. Thus, many “hybrid” flood protection measures are being developed and are valued upon since a mature vegetated foreshore can significantly reduce wave energy by depth-induced wave breaking, bottom friction, and attenuation by vegetation itself (Sutton-Grier et al., 2015). We say mature since seedlings cannot provide the same level of protection as a fully-grown tree. Figure 1.2 depicts various combinations of hybrid flood protection schemes, including minimal defence (top), natural measures (second from top), managed realignment (second from bottom) and hybrid defence measures (bottom). Since vegetation reduces wave heights at the coastline, a dike of lesser height can be built to accommodate this reduction of wave heights. In the figure, salt marsh can also be read as mangroves. These hybrid schemes lead to an overall decrease in construction costs. These are explored in more detail by Tusinski (2012) and Tas (2016).

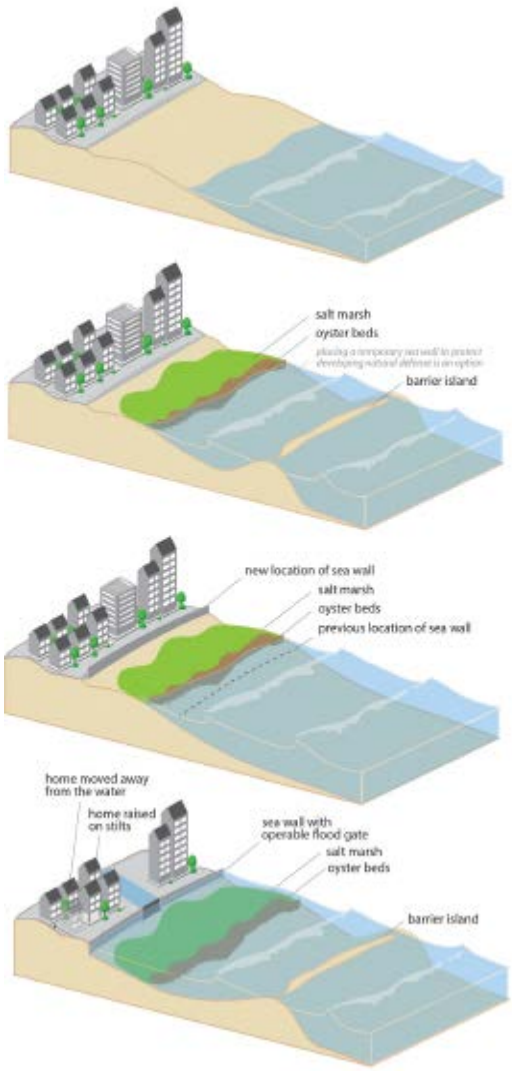

Figure 1.2: Coastal defence examples (Sutton-Grier et al., 2015)

1.2. Motivation and Research Significance

Hydraulic forcing from extreme events is a large risk around the global coastlines. It is known that mangroves help in attenuating waves, but currently, there is a lack of efficient and accurate analysis of this fact on a large scale. There has been a lot of localised studies on the beneficial engineering effects of mangroves (for example by Narayan (2009) and Harihar (2015)).

Moreover, a lot of numerical models have been developed that predict wave dissipation in mangrove forests. Those like Dynveg can model highly flexible vegetation interaction with hydrodynamics (Dijkstra & Uittenbogaard, 2010). However, these models lack validation. The validating observations are determined from laboratory measurements which are on a small scale, and from field measurements which are not on the scale. The problem on the field scale is that not many field measurements are available to validate with.

If more proper knowledge is obtained on how the models predict the wave transformation and dissipation, especially in the foreshore, then those can be used to predict reliable results leading to efficient dike designs, for example, in the case of a nature-based or hybrid flood protection design. Tang et al. (2017) showed in a numerical model study that the wave run-up levels significantly reduced due to the presence of vegetation. Reduced wave heights, wave run-up, and wave overtopping will ultimately lead to a reduction of dike heights. A lower dike is also a narrower dike. When assuming a slope of 1:3 at both sides, the lowering of a dike by 1 m will lead to the footprint of the dike becoming narrower by 6 m.

This thesis study tries to bring more clarity into the model-lab relationship and get an insight on how accurate these models are to predict wave transformation and attenuation. Once this insight is achieved, it can be extended to the more complicated conditions of vegetation presence.

1.2.1. Objective

To properly assess the effectiveness of the models, the following research question is posed:

> ***How can we, to a certain degree of accuracy, determine how the waves behave and transform at a coast, that is typically vegetated?***

To answer the main question, the following sub-questions need to be answered:

- How do waves behave on a foreshore, that is generally found on tropical vegetated coastlines?
- What is the necessity of the used models?
- How do the models behave on theoretical conditions?
- How do the results obtained from laboratory tests match up with the predicted model results?
- Conversely, how do the models predict the results when inputted with the laboratory conditions?

In the process of answering these questions, we hope to bridge the gap between the development of models and its applicability to the wave properties' prediction on shallow foreshores.

1.3. Research Approach and Thesis Structure

The thesis is divided into five chapters and four appendices. Chapter 1 describes the motivation, research significance, and general approach to the study.

Chapter 2 introduces the reader to a brief theory behind the waves and wave transformation, in the oceanic waters and in the coastal waters, and briefly touches on the processes behind the transformation.

Chapter 3 gives a clue of the models used in coastal engineering and then focuses on models used in this research along with a few benchmark tests. This provides an idea of the behaviour of specific wave types on the shallow foreshores.

Chapter 4 presents the main results obtained from the validation tests. The validation tests comprised of inputting the surface elevation data as-is, a corresponding filtered data, and a laboratory-condition-replicating input.

Chapter 5 explains the discussions, conclusions from the validation tests, limitations, and recommendations for further study.

The appendices present the model scripts as well as input conversion and its sensitivity analysis.

2
BACKGROUND

I know one thing; that I know nothing.
Socrates

This chapter introduces waves and the processes involved in the coastal zone. A grasp of the theoretical background is necessary, as always, before tackling a problem. This chapter covers the offshore and nearshore hydrodynamics that one must consider while solving a problem regarding waves.

2.1. Waves

Wave, the definition of which may seem insignificant, but many people consider waves to be any sea-surface elevation. However, there is a difference between surface elevation and wave.

A *surface elevation*, in a time record, is the instantaneous elevation of the sea surface relative to a reference level. A *wave*, however, is a profile of the surface elevation between two successive zero-crossings, where 'zero' means the average of surface elevations (Holthuijsen, 2007). One can either consider two consecutive upward zero-crossings or two consecutive downward zero-crossings to get a wave. However, downward zero-crossings are preferred (J. Bosboom, personal communication, March 2016) because:

- they relate more directly to visual observations of wave heights where the wave height is taken to be the height of the crest relative to the preceding through, and
- the front face of the waves is included between two downward zero-crossings, and this is often more relevant than the back face, for example, in wave breaking studies.

2.2. Wave Propagation in Oceanic Waters

Here, oceanic waters mean deep waters, i.e., where the waves are not affected by the bottom. The waves are also not affected by obstacles, such as headlands, islands, and breakwaters.

2.2.1. Description of Waves

Waves are generated by air-pressure fluctuations at the sea surface due to a constant wind (i.e., constant in space and time). This is the *idealised* condition. The growth of the sea state depends on the wind speed, how long the wind blew (duration), and over what length the wind blew (fetch). This results in *young sea states* (when the waves grow at short fetches) and afterwards, *fully developed sea states* (when the wave growth stops, due to a balance of energy transfer from the wind to waves and wave breaking). The wave

parameters like the significant wave height and the period are also dependent on the above factors.

Three-dimensional wave spectrum describes the sea states, the surface elevations being represented by wave number *k*, angular frequency *ω*, and direction *θ*. However, since *k* is related to *ω* through the dispersion relationship ($\omega^2 = gktanh(kd)$; *d* is water depth), the three-dimensional spectrum reduces to a two-dimensional spectrum, otherwise known as the *frequency-direction spectrum* after it is converted from a discrete amplitude spectrum into a continuous variance density spectrum. It is represented below (in terms of absolute frequency *f* and direction *θ*):

$$E(f,\theta) = \lim_{\Delta f \to 0} \lim_{\Delta \theta \to 0} \frac{1}{\Delta f \Delta \theta} E\left\{\frac{1}{2}\underline{a}^2\right\} \quad (1)$$

E(*f*,*θ*) has units of m^2/Hz/degree or m^2/Hz/radian, following all the defining constituents being in S.I. units.

The one-dimensional *frequency* spectrum E(*f*) is obtained by removing the directional information from the frequency-directional spectrum E(*f*,*θ*), i.e., by integration over all directions (per frequency):

$$E(f) = \int_0^{2\pi} E(f,\theta) d\theta \quad (2)$$

The one-dimensional frequency spectrum has a universal shape: the JONSWAP[1] spectrum for young sea states or the Pierson-Moskowitz spectrum for fully-developed sea states. The JONSWAP spectrum is usually shape-stabilised for wind waves, because in deep waters, in an *arbitrary* condition, the nonlinear wave-wave interactions (quadruplets) redistribute the wave energy over the spectrum but do not result in the addition of or removal of energy from the spectrum. Thus, in the engineering community, it is widely accepted as a design spectrum.

The waves degenerate into *swell*, as they move away from their generation location, because of direction- and frequency-dispersion. Thus, the JONSWAP spectrum does not remain a representative of the swell spectrum. Figure 2.1 shows typical JONSWAP and Pierson-Moskowitz spectra. Figure 2.2 represents a typical wave spectrum found in the North Sea, off the Dutch coast, which is usually a mixture of swell and wind waves.

A good way to describe the waves is the so-called significant wave height or H_s. In the *time domain*, this is the mean of the highest one-third of waves in the wave record. Mathematically, it is as follows:

$$H_s = H_{1/3} = \frac{1}{N/3} \sum_{j=1}^{N/3} H_j \quad (3)$$

where j = 1 means the highest wave, j = 2 is the second-highest wave, and so on, N is the total number of waves.

[1] Acronym for JOint North Sea WAve Project, by Hasselmann et al., 1973

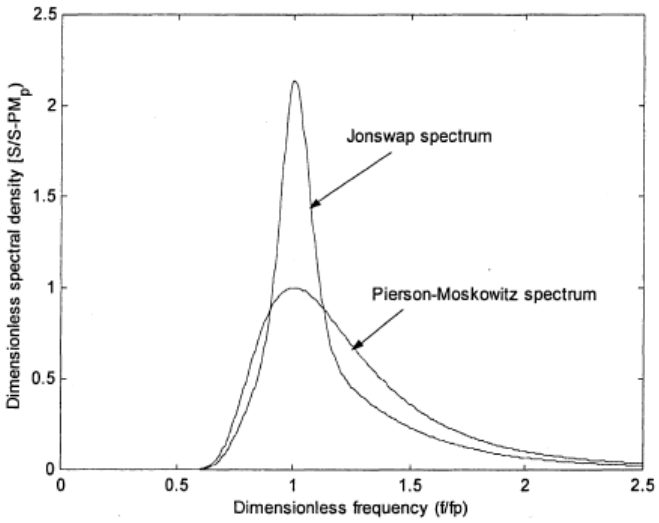

Figure 2.1: JONSWAP and Pierson-Moskowitz spectrum (NTNU TBA4265 Compendium, 2016)

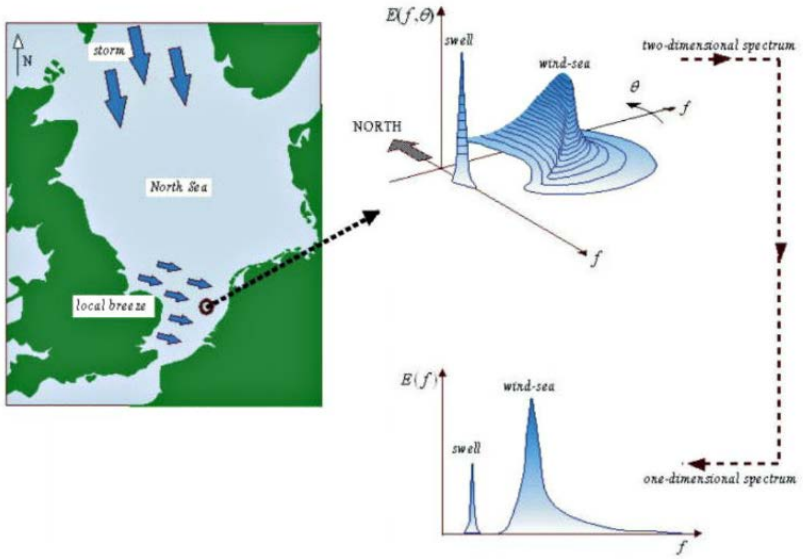

Figure 2.2: A wave spectrum off the Dutch coast (Bosboom & Stive, 2015)

In the *frequency domain*, it is defined in terms of the variance m_0[2] or standard deviation σ_η of the surface elevation:

$$H_s = H_{m_0} = 4\sqrt{m_0} = 4\sigma_\eta \quad (4)$$

Just one value apparently determines the strength of the storm considered. However, for irregular wave conditions, the Rayleigh distribution will not be applicable anymore, as the highest waves will start breaking first. For such a condition, a quadratically weighted and averaged value, the so-called root-mean-square wave height (H_{rms}) is a good description of the wave height statistics:

$$H_{rms} = \sqrt{\frac{1}{N}\sum_{m=1}^{N} H_m^2} \quad (5)$$

[2] The subscript '0' indicates that it is the zeroth-order moment (area) of the wave spectrum.

where m is the individual wave height, and N is the total number of waves.

2.2.2. Linear Wave Theory

The *Linear Wave Theory* governs the propagation of waves in oceanic waters. This theory, also known as Airy[3] wave theory, is based on only two equations: a *mass* balance equation and a *momentum* balance equation. It defines the free surface elevation (η) of a propagating harmonic wave in oceanic waters (in the positive *x*-direction) as follows:

$$\eta(x,t) = a\sin(\omega t - kx) \qquad (6)$$

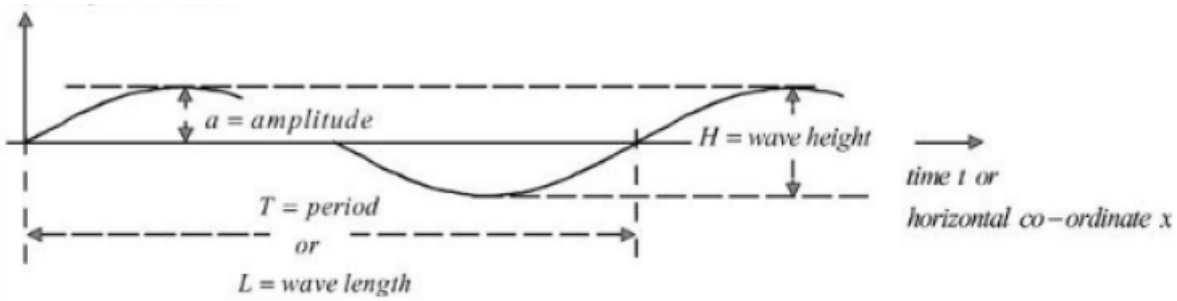

Figure 2.3: Propagating harmonic wave with its parameters (Holthuijsen, 2007)

A typical propagating harmonic wave is shown in Figure 2.3. The propagation of the wave is best observed by fixing an observing point to the crest of the wave and following it as it propagates. The fluid particles below the water surface follow an orbital path. This path, however, changes shape as the wave progresses from deep water to intermediate water to shallow water. This is because of the change in vertical displacement as the wave travels toward shallow waters as well as with increased depth from the surface. The orbital path, as a result, changes into an elliptical shape, and finally, only horizontal to-and-fro motions at the bed in shallow water. This is shown in Figure 2.4.

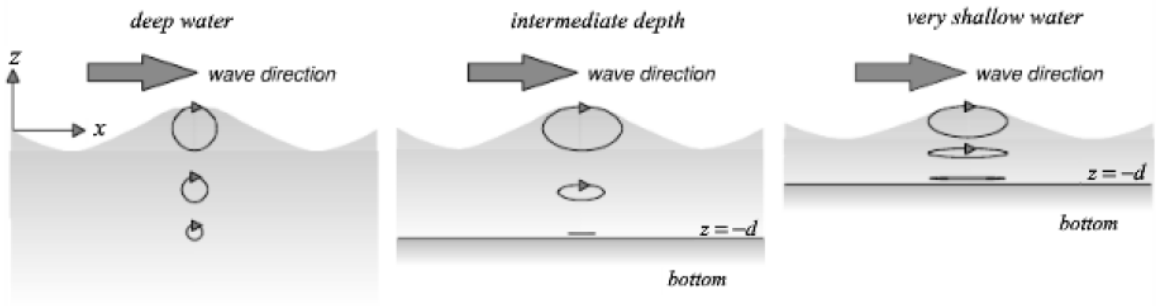

Figure 2.4: Orbital motion in deep, intermediate, and shallow waters (Holthuijsen, 2007)

2.3. Wave Propagation in Coastal Waters

Coastal waters refer to shallow waters, where the water is shallow enough to affect the waves. The waves start feeling the bottom surface. The energy balance is tried to be maintained while the waves propagate into shallow zones. This balance is achieved by various nearshore hydrodynamic processes, such as refraction, shoaling, and diffraction. The first two are caused by changes in horizontal variations in water depth, while horizontal

[3] Named after George Biddell Airy (1801-1892), an English mathematician, who published this theory in the 19th century.

variations in amplitude cause diffraction. These processes lead to a transformation in waves, in other words, there is a change in wave height, length and direction.

2.3.1. Processes in the Coastal Zone

The variation of waves in their direction of propagation is called *shoaling*. It is caused due to depth-induced changes of the group velocity in the wave propagation direction. Wave heights increase as the propagation continues, because of energy concentration.

Refraction of waves is the turning of waves towards shallower water due to changes in phase speed in the lateral direction. Snell's law[4] is used to compute the harmonic wave direction for parallel depth contours. If the contours are not parallel, wave rays should be utilised instead.

Diffraction of waves is also the turning of waves, but this turning is towards areas with lower amplitudes, due to amplitude changes along the wave crest. This phenomenon is usually strong along the shadow line of obstacles, like headlands and breakwaters. The Huygens-Fresnel principle[5] can be used for computing the diffraction pattern.

Reflection is the phenomena when a long-crested harmonic wave reflects off an obstacle, with or without losing any energy. This can create a standing wave.

Wave-breaking happens when the wave becomes depth-limited. A wave crest becomes unstable as it becomes too steep and starts breaking when the particle velocity exceeds the speed of the wave. This occurs at an H_s/d ratio (otherwise known as the *Breaker index*) of approximately between 0.78 and 0.88 (Bosboom & Stive, 2015). Chella et al. (2015) have proposed that the milder slopes slow down the wave breaking, i.e., make the breaking point move shoreward, by increasing the length over which the waves shoal. This proposition is also confirmed by Tas (2016).

Set-up happens near the shoreline because there has to be a conservation of momentum, not only energy. The set-up is the wave-induced rising of the mean water level as the waves propagate towards the coast.

Surface rollers are generated by breaking waves, which can be observed as the foam layer in the breaker zone, serving as a temporary storage of energy and momentum. After the breakpoint, the wave energy is first converted into turbulent kinetic energy, thereafter completely dissipated by producing turbulence (Bosboom & Stive, 2015).

2.3.2. Wave Transformation

As the waves propagate towards shallow water, various processes occur, and the energy gradually dissipates, in the form of wave dissipation and white-capping. These processes are linear wave propagation effects (like shoaling and refraction) and nonlinear transformation of wave shape (skewness and asymmetry). The nonlinear wave transformations are important to consider because they play a role in particle transport, unlike in deep water where there is no net particle movement.

[4] Named after the Dutch astronomer and mathematician, Willebrord Snellius (born Willebrord Snel van Royen) (1580-1626)

[5] Named after the Dutch physicist Christiaan Huygens (1629-1695) and the French physicist Augustin-Jean Fresnel (1788-1827)

Skewness is the gradual steepening of the wave crest and flattening of the wave trough (thus an asymmetry in the horizontal axis). *Asymmetry* is the pitching-forward shape of the wave, as the wave steepens before breaking (thus an asymmetry in the vertical axis). These nonlinear transformations, while the wave is evolving, cannot be described by Airy wave theory and therefore done by theories such as Stokes' theory and Boussinesq equations.

Figure 2.5 summarises the applicable ranges where different theories can be applied based on the wave and profile properties.

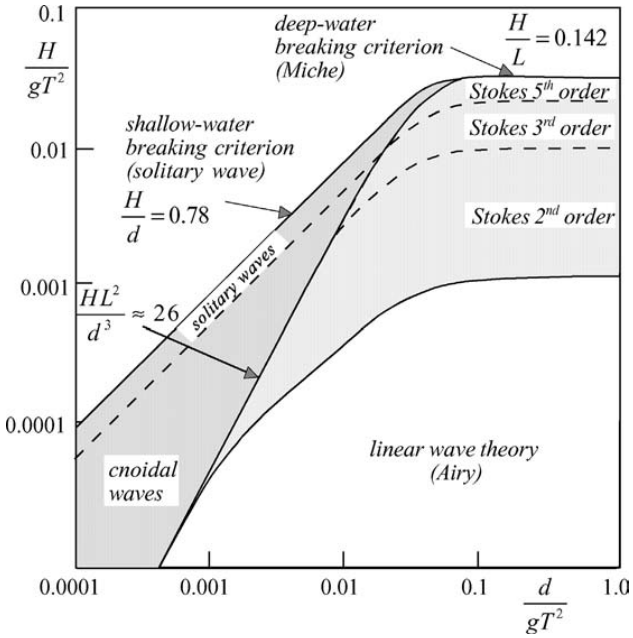

Figure 2.5: Ranges of applicability of the various theories (Holthuijsen, 2007)

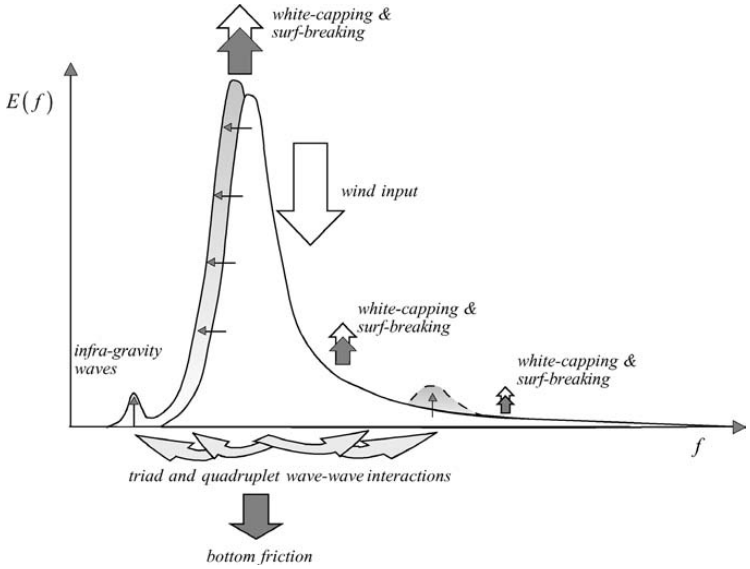

Figure 2.6: The energy flow through the spectrum in shallow water (Holthuijsen, 2007)

As the waves evolve, i.e., propagate in the coastal waters, the energy peak decreases due to various processes. Figure 2.6 depicts this in a single figure, with the relevant source terms. One thing to be noticed is that white-capping and the triad and

quadruplet wave-wave interactions make the energy shift to the lower and higher frequencies.

Table 2.1 summarises the mentioned processes and its relative influence on the wave height in different water depths (adapted from Janssen (2016)).

	Oceanic waters	Coastal waters	
		Shelf seas	Nearshore
Wind generation	+++	+++	+
Quadruplet wave-wave interactions	+++	+++	+
White-capping	+++	+++	+
Bottom friction	0	++	++
Bottom refraction/shoaling	0	++	+++
Depth-induced breaking	0	+	+++
Triad wave-wave interactions	0	0	++
Diffraction	0	0	+

Table 2.1: Relative importance of processes on waves for oceanic and coastal waters (+++: very important, ++: important, +: weakly important, 0: unimportant)

3
MODELS

If the only tool you have is a hammer,
you treat everything as if it were a nail.
Abraham Maslow

This chapter briefly introduces the numerical modelling concepts used in coastal engineering. Moreover, it further explains the models applied in this research, SWAN and SWASH, along with their model set-up and initial results.

3.1. Numerical Modelling Concepts in Coastal Engineering

For prediction of nearshore hydrodynamics, there are usually three modelling concepts present, differentiated on the detail of the hydraulic forcing.

3.1.1. Wave Averaged Modelling

Wave averaged modelling is the standard way of modelling waves in coastal engineering. The wave energy does not fluctuate on the timescale of days, but it is constant over the timescales of thirty minutes or so. The mean shoaling and wave-breaking is observed. This modelling approach is a fast approach. It is hard, however, to include the detailed processes near the waterline, as short wave and long wave run-up are not included explicitly. Examples of such models are ‘standard’ Delft3D and SWAN.

3.1.2. Short-wave Averaged, Long-wave Resolving Modelling

These types of models compute the wave energy on a wave group timescale and do not resolve the individual short waves. The wave breaking does not take place on a single wave timescale but on wave group timescale. This approach has the benefit that it can include effects of long-wave motions and is computationally less demanding than the short-wave resolving approach. Examples of such models are Delft3D (‘Long wave option’) and XBeach.

3.1.3. Short-wave Resolving Modelling

These models resolve the short-wave motion such that every single wave is simulated. This enables to observe the intra-wave velocities and sediment transport. The nonlinear transformations (skewness and asymmetry) can also be computed. However, it is computationally costly, as small time step and grid size are required. Using this modelling approach is necessary when computing parameters that depend on short-wave characteristics, such as overtopping, run-up, or wave propagation in harbours. Examples of such models are Boussinesq models (Funwave, Triton) and SWASH.

3.2. Model Requirements

What has to be modelled? This question can be answered from the thesis title: waves on shallow foreshores. This title has significance because not much research has been done on shallow foreshores and the wave behaviour on them (Tas, 2016).

How do the waves need to be modelled? A choice of a model needs to be made based on the requirements and the output desired. The requirement is a model that can provide an insight into the hydrodynamics in the shallow foreshores. The model should be able to model the wave transformation from offshore to nearshore and up to the shoreline, considering different dissipation mechanisms, especially on shallow gentle foreshores. The scope of this research does not include the morphodynamics. Nonetheless, it is beneficial to use a model which looks into that as well, because it will be easier to put this model into further research on morphodynamical aspects.

Two candidate models are chosen for this research – SWAN and SWASH. These offer two different approaches to the same problem, one being a wave averaged (phase-averaged) model and the other being a short-wave resolving (phase-resolving) model. These models also consider the vegetation effects (SWAN was used by Suzuki et al. (2011) to model wave dissipation by vegetation), thus are likely candidates when the hydrodynamics and the morphodynamics in the mangrove areas are considered, thus eventually contributing to coastal implementations, like mangrove preservation programs, dike realisations, or beach nourishments to protect hinterland and coast.

The primary reason to use SWASH is that it is a time domain model which solves the nonlinear shallow water (NLSW) equations. The importance of a time domain model is that it can simulate the low-frequency waves which have been found to be important in wave propagation in vegetation (Phan et al., 2011).

3.3. Bathymetric Profile

In order to test the models for a shallow foreshore condition, there has to be such a profile. An experiment[6] was conducted in the TU Delft Laboratory of Fluid Mechanics flume, replicating such a profile and measuring the wave data. The data will be introduced later in Chapter 4. Figure 3.1 shows the bathymetric profile that has been used in the flume. The profile is representative of a shallow foreshore condition, replicating a reef condition, i.e., the shallow part is completely flat and has no slope. However, this can also be taken as a test case for a coast with mangrove forests, which tend to have very long and gentle foreshores. The scale used in the laboratory is 1:20. To measure the depths, a laser scanner was used. The scanner took the depths every 5 cm along the whole length of the flume. The length of 37.7 m was covered in 754 data points. The relatively steep portion in the profile with 1:10 slope, i.e., data points from around 200 to 300 is not present at a real mangrove coast, but included here because the flume is otherwise not long enough.

[6] The experiment was conducted by Jochem Dekkers as part of his M.Sc. thesis research on physical and numerical modelling of undular bores on fringing reefs, supervised by Dr. Marion Tissier.

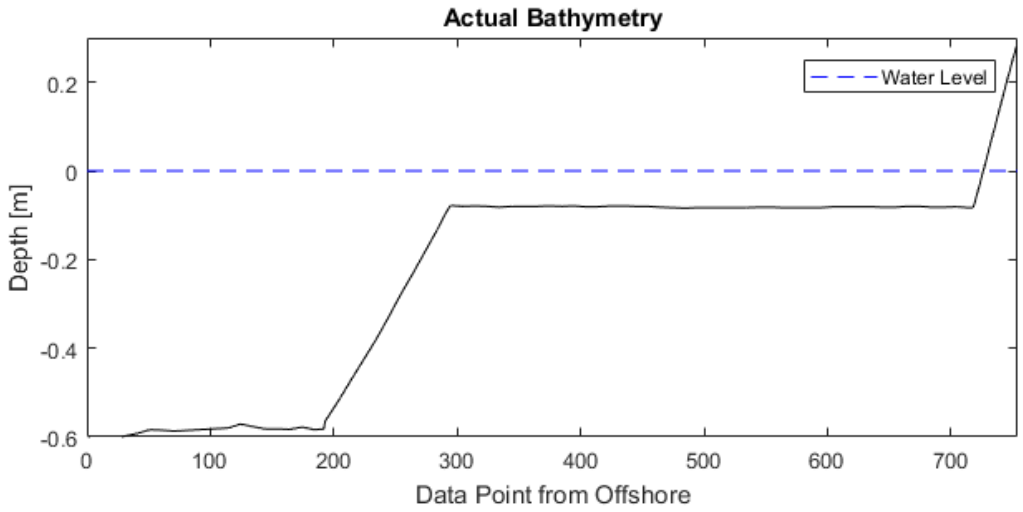

Figure 3.1: Actual Bathymetry, used in the laboratory

However, as such an accuracy is not required, the profile was schematized as shown in Figure 3.2 below. The undulations were removed; the offshore depth was kept constant at 60 cm, then with a slope of roughly 1:10, the depth decreases until 8 cm. Then for a length of 21.1 m, the depth remains constant at 8 cm. After this, with a 1:5 beach slope, the depth decreases up to zero and increases up to 30 cm above water level. The horizontal distances are taken such that the '0' value is at the foreshore tip. The still water level is at '0' on the vertical scale.

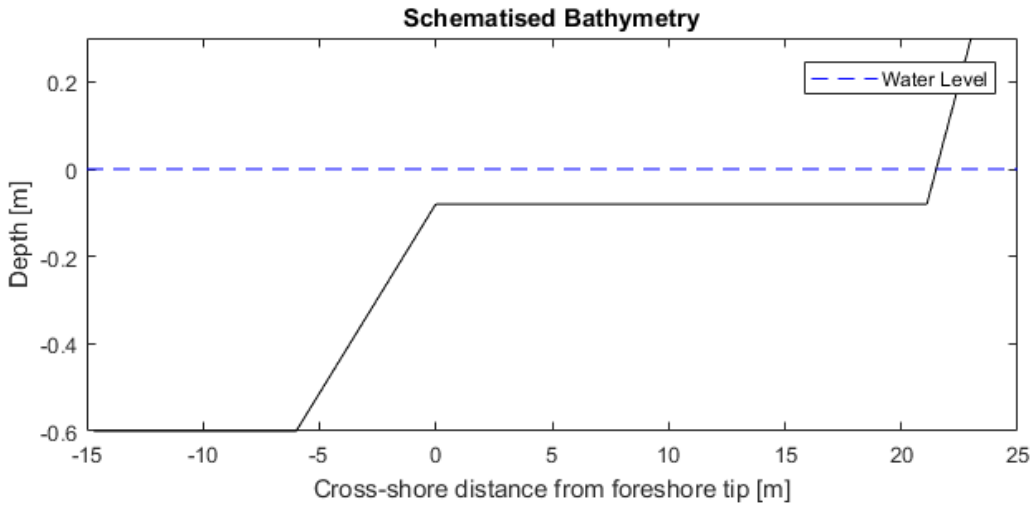

Figure 3.2: Schematized Bathymetry used in modelling

The above bathymetry was written with the help of 378 grid points (such that the number of grids is 377 and grid spacing is 10 cm) into a bottom file (*.bot*) to be used in the models. It is to be noted, however, that both SWAN and SWASH read positive bottom values as below water and negative values as above water. Therefore, the signs of the values are inverted before writing them into a bottom file, or alternatively, the model input file is written in such a way that a multiplication factor of -1 is included while reading the depth values.

3.4. SWAN

3.4.1. Model Description

SWAN is the acronym for Simulating WAves Nearshore. It is a third-generation[7] spectral wave averaged model, developed by the Delft University of Technology, for obtaining realistic estimates of waves in coastal and inland waters. It transforms the offshore wave conditions into nearshore wave conditions, taking a variety of processes into account. The relevant physical processes that SWAN takes into consideration are wind-wave growth, white-capping, bottom friction, depth-induced wave breaking, dissipation due to vegetation, mud or turbulence, obstacle transmission, nonlinear wave-wave interactions (quadruplets and triads), and wave-induced set-up (The SWAN Team, 2016). These parameters can be activated as per the user's wish, depending on the situation. SWAN can run in a first, second or third generation mode, as well as in one-dimensional, for instance, to replicate a lab-flume situation, or in two-dimensional mode, for example, to replicate a basin situation.

SWAN does not calculate wave-induced currents. This limitation can be overcome by adding the currents as an input from a circulation model. Another limitation is its lesser efficiency in oceanic scales when compared to, for instance, WAVEWATCH III[8]. On the plus side, it is computationally fast and saves time, especially when it is run in the stationary mode.

3.4.2. Model Set-up

SWAN was run in a stationary mode and in one-dimensional mode (to be representative of the flume situation, i.e., one cross-section). This was also warranted, because in the flume, two-dimensional effects, such as refraction and diffraction, can usually be neglected.

The length of the computational domain is the same as the input domain, that is the whole length of the bathymetric profile. The computational grid was a regular grid with a grid size of 10 cm or 0.1 m, i.e., equal to the input grid size. The wind-wave growth cannot be neglected in such a shallow foreshore. However, since there is no wind in the laboratory, the wind parameter is not included in the model.

At the offshore boundary, the default wave spectrum is imposed. This spectrum is a standard JONSWAP-shape spectrum, with a peak enhancement factor γ of 3.3, and the directional width expressed in terms of power *m* itself in the distribution function $cos^m(\theta - \theta_{peak})$.

The wave direction is perpendicular to the shoreline, onshore directed. At the landward boundary, a closed boundary was defined. However, this will have no effect on the results, since the waves of around 0.03 m will never reach z = +0.3 m. The water level is set at zero, since there is no change in the water levels in the laboratory. This might be

[7] In the first-generation models, nonlinear wave-wave interactions are not included. The second-generation models only parametrise these non-linear interactions, while third-generation models explicitly include all non-linear wave-wave interactions, and it is up to the user to specifically exclude these interactions, depending on the outcome wanted.
[8] A wave forecasting model of National Oceanic and Atmospheric Administration (NOAA), USA

changed in a real-life scenario, when water levels based on tides and return periods are included.

SWAN was run in the third-generation mode for this lab condition. The nonlinear wave-wave interactions and diffractions were not considered. However, others, like white capping, depth-induced wave breaking (can be specifically switched off, otherwise always considered), triad wave-wave interactions, bottom friction, and setup are considered. Vegetation and mud are not considered, as they are not present in this situation. For all values, the default settings are applied. A more detailed SWAN code walkthrough is provided in Appendix A.

3.4.3. SWAN Model Analysis

For the analysis of the model performance, the so-called benchmark tests, two offshore boundary conditions were imposed. These values were consistent with the overall scale of the model, i.e., 1:20.

- A regular wave with a wave height (H) of 0.07 m and a wave period (T) of 2 s.
- A bichromatic[9] wave with component wave heights of 0.06 m and 0.08 m, and wave periods of 1.5 s and 2.5 s.

Why a bichromatic wave? This is because, in most of the tropical coasts, the incoming waves are generally a mix of swell and wind conditions. While wind condition is irregular, swell is usually consistent. This bichromatic wave tries to replicate this swell condition, even if it is very theoretical and has two peaks side-by-side which is not found in a field spectrum.

The regular wave input was put into the model in two ways:

- Parameters, i.e., single numerical values for wave height and wave period.
- A variance density spectrum of the corresponding wave parameters.

The bichromatic wave was put as input by means of a spectrum. For more information on this, the attention of the reader is directed towards Appendix C and D. The wave direction was inputted as per the nautical[10] convention used in the SWAN model, i.e., 270° - from the West.

Both the SECTOR and CIRCLE option were evaluated in the computational grid for the spectral wave direction because it was a known fact that waves do not come with a spectral distribution over a full circle in a lab condition. However, trying to do a trade-off between a real condition and a lab condition, a directional spreading of 30° was used, which should be 0° in the lab. Thus, the range of direction was 240° to 300° (as waves are coming at 270° w.r.t. North).

It is important to note, however, that the author mentions the output results on the y-axis of all the results figures as Significant Wave Height – H_s. This is because that is what SWAN and SWASH give outputs for, as it is an important design parameter. However, for regular waves, H_s is the same as H, by definition, as there is only one H value. For

[9] Bichromatic wave means a wave consisting of two sinusoidal waves, superimposed (visual representation of such wave in Figure 4.2).
[10] Nautical convention means the directions are noted with respect to the true North and it is considered the direction the winds and waves are coming from.

bichromatic waves, it is hard to establish a H_s value, but the maximum H value will supposedly be the addition of individual wave heights (following the linear superposition principle) when the components are in-phase with each other.

3.4.4. Results

The computed values give quite the expected results. They are presented in the figures below. Figure 3.3 shows the results of the regular wave case when the input was in the form of parameters (left) and in the way of a spectrum (right). Figure 3.4 shows the results of the bichromatic wave case. Figure 3.5 and Figure 3.6 show the results for all the SWAN performance runs, for the Circle and Sector grid, respectively.

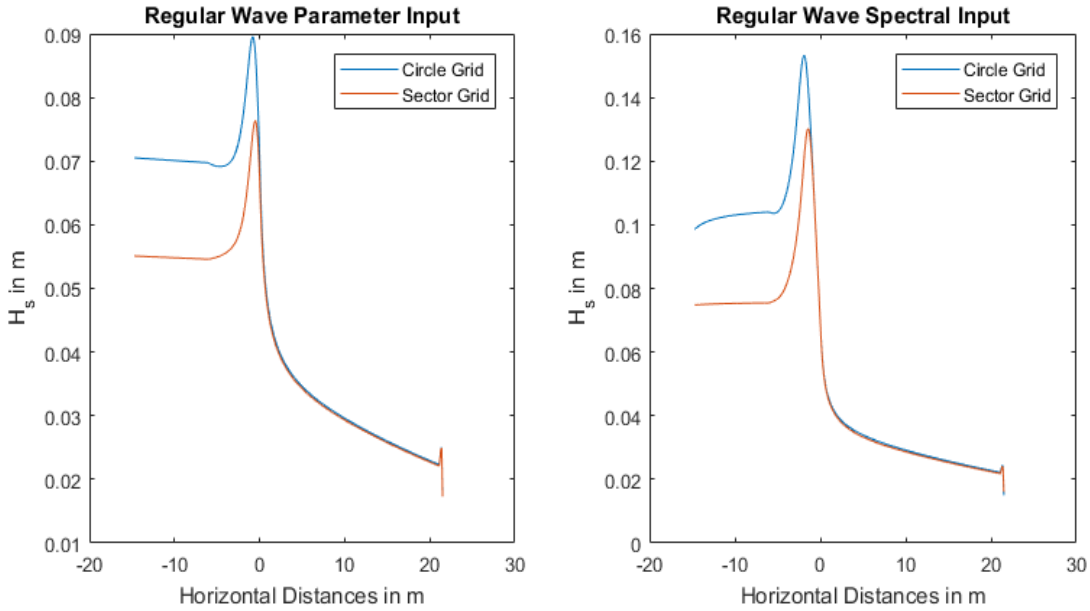

Figure 3.3: SWAN Regular Wave case (Parametric and Spectral Inputs)

3.4.4.1. Regular Wave – Parametric Input

The wave heights are as expected. In the circular grid, the waves have the same value at the offshore location as the input parameter. In the sectoral grid, however, the output at the offshore location was lower than that. This reduction of value can be attributed to the fact that wave height is not considered as-is by SWAN, but is taken as an energy input. For a sectoral directional space, SWAN considers the boundaries as fully absorbing (SWAN Scientific and Technical Documentation, 2016). This leads to free propagation of energy out of the boundary resulting in some loss of energy to the directional space outside the sector.

3.4.4.2. Regular Wave – Spectral Input

The starting wave height is in the order of 1.4 times of the H_s in the parameter case (attention directed towards Figure 3.5 and Figure 3.6). In the sectoral grid, for the same reason, there is an overall decrease of wave heights. There is a rapid steepening of the waves compared to the parametric input case. This might be due to how SWAN deals with the type of input. When given as a parametric input, H_s is considered in a time domain ($H_{1/3}$). When given as a spectral input, it is considered in a frequency domain (H_{m_0}).

3.4.4.3. Bichromatic Wave

Since SWAN is not able to handle two regular wave parameters simultaneously to consider it as a bichromatic wave[11], a spectral input was used for the bichromatic wave. There is no energy loss in the circular grid compared to the sectoral grid. However, in the circular grid, it appears that the wave heights increase in the offshore region, then slightly decrease, before shoaling starts to occur. This is not observed in the sectoral grid.

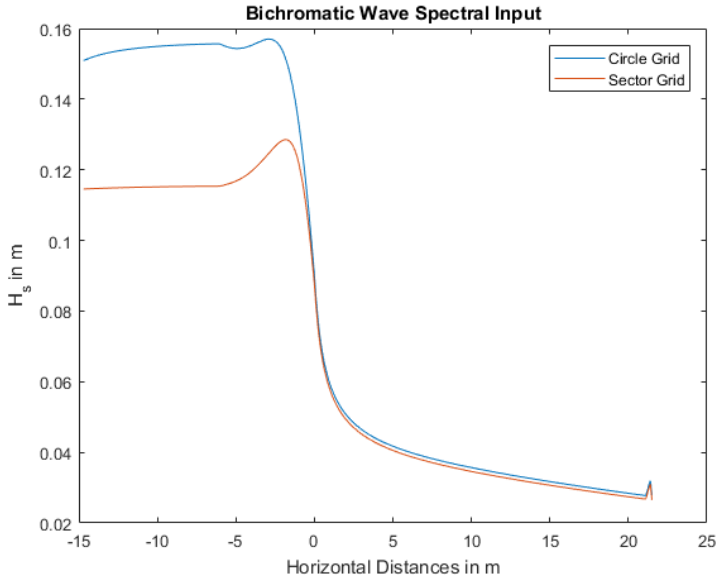

Figure 3.4: SWAN Bichromatic Wave case

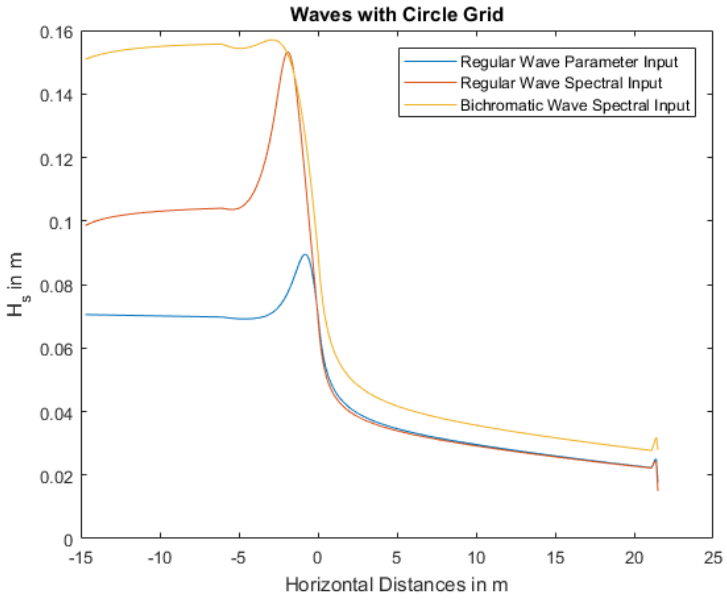

Figure 3.5: SWAN outputs with various conditions (Circle Grid)

[11] The author tried to input two consecutive regular waves. It resulted in one of the components being ignored, resulting in the supposedly bichromatic wave being treated as a regular wave.

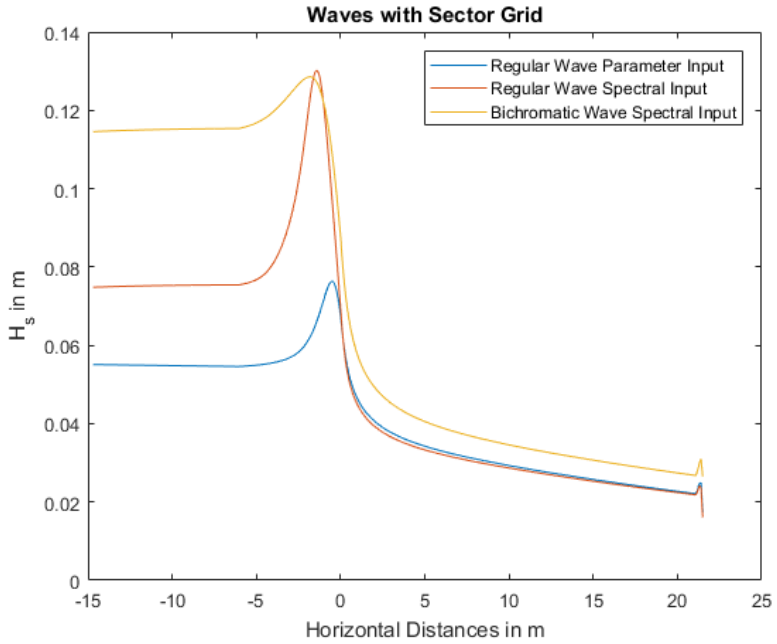

Figure 3.6: SWAN outputs with various conditions (Sector Grid)

3.4.4.4. Common Observations

- When both the regular and bichromatic cases are considered simultaneously, the wave heights are higher in the bichromatic case than the regular case.
- The computational time was significantly more in the sector case than the circle case.
- In the foreshore or shallow region, there is hardly any difference in the wave heights in any case (circle/sector, parametric/spectral). It is only different in the case of changing wave conditions (regular/bichromatic).
- Wave breaking occurs a bit before in the case of the circle than in the case of the sector grid. The wave height is higher in the case of a circle, thus resulting in earlier steepening and breaking of waves.

3.5. SWASH

3.5.1. Model Description

SWASH is the acronym for Simulating WAves till SHore. It is a non-hydrostatic, phase resolving wave-flow model, developed by the Delft University of Technology, which can also be used to simulate irrotational flows and transport phenomena in one, two or three dimensions. (The SWASH Team, 2017) The fluid layer can be depth averaged or multi-layered. SWASH can be used for simulating wave transformation in surf and swash zones, complex changes in rapidly varied flows (dike breaking and coastal flooding), density-driven flows and large-scale oceanic circulation. SWASH is essentially applicable in the coastal regions up to the shore.

The fact that SWASH is a non-hydrostatic model makes it unique. At offshore depth, the hydrostatic pressure assumption is valid. Near shore, when the non-hydrostatic pressure term becomes necessary, SWASH makes use of the full vertical momentum equation. Unlike other Boussinesq-type wave models, SWASH improves its frequency

dispersion by increasing the number of vertical layers instead of increasing the order of derivatives of the dependent variables. This makes it faster and robust, compared to those models.

In principle, SWASH can capture flow phenomena with spatial scales from centimetres to kilometres and temporal scales from seconds to hours. On the downside, since it takes a phase-resolving approach, it is computationally very demanding and time-consuming.

3.5.2. Model Set-up

SWASH was used in a one-dimensional mode in this research for all runs, as in the case of SWAN. The computational grid was also a regular grid, and the grid size was also kept similar, i.e., 10 cm. As initial conditions, the water level and velocity components were set to zero. An appropriate spin-up time was included.

The wave direction is perpendicular to the shoreline, onshore directed. The offshore boundary was set as weakly reflective. At the landward boundary, a closed boundary was defined. However, this will not affect the results, since the waves of around 0.03 m will never reach z = +0.3 m. The water level is set at zero, since there is no change in the water levels in the laboratory. This might be changed in a real-life scenario, when water levels based on tides and return periods are included.

Momentum must be conserved everywhere, and upwind discretization was used for the momentum equations. Explicit time integration was applied, where the Courant number is limited between 0.1 and 0.5, which is advised in case of nonlinearities.

A single depth-averaged layer was chosen because it was as such in the laboratory. Vegetation and mud effects were excluded. However, normal bottom friction was included, with the default values. The non-hydrostatic mode was activated.

A smoothening time of 5 seconds was taken. Normally it should be around 1-2 times of wave period. Adding this prevents instability while starting the model run (M. Zijlema, personal communication, April 2017). A more detailed SWASH code walkthrough is provided in Appendix B.

3.5.3. SWASH Model Analysis

For the analysis of the model performance, two offshore boundary conditions were imposed. These were the same as in the SWAN model. There must be a duration specified, over which the significant wave height is calculated.

- A regular wave with a wave height (H) of 0.07 m and a wave period (T) of 2 s.
- A bichromatic wave with component wave heights of 0.06 m and 0.08 m, and wave periods of 1.5 s and 2.5 s.

The default input parameters for SWASH are significant wave height and peak wave period. The same clarification, as in SWAN case, applies here.

SWASH allows the input of two wave components of a bichromatic wave in a Fourier series. The parameters required are the zero-frequency amplitude (here taken as 0 m) and

the individual amplitudes (m), angular frequencies (rad/s), and phase (degrees) of the different components.

Unlike SWAN, there is no Circle or Sector grid, because SWASH is a time-domain model. Thus, the concepts of direction and directional spreading within a spectrum is moot. Running SWASH in non-stationary mode is, thus, mandatory.

3.5.4. Results

3.5.4.1. Regular Case and Choice of Run Time

In the normal wave case, the output varied depending on the computational period. Thus, insight was obtained on how it affects the output. Figure 3.7 shows the said dependency. As seen, the output stabilises more or less after a run of 12 minutes. In fact, there is hardly any difference between the run of 12 minutes and 1 hour and 20 minutes, and the graphs coincide.

This computational period is the summation of the spin-up time and the duration over which the surface elevation is averaged to obtain the significant wave height. For the regular wave, the normal spin-up time is around 5 minutes[12]. However, for the different runs with different computational periods as in Figure 3.7, the spin-up time was varied, so that the duration over which the significant wave height was calculated is not too short and is consistent with the other runs.

This spin-up time can be seen as the time difference between the application of the initial and the boundary condition (M. Zijlema, personal communication, April 2017). In terms of waves, the spin-up time can be expressed as the first 100 - 200 waves. These are also seen as sacrificial waves, that is waves from which any information is not to be considered.

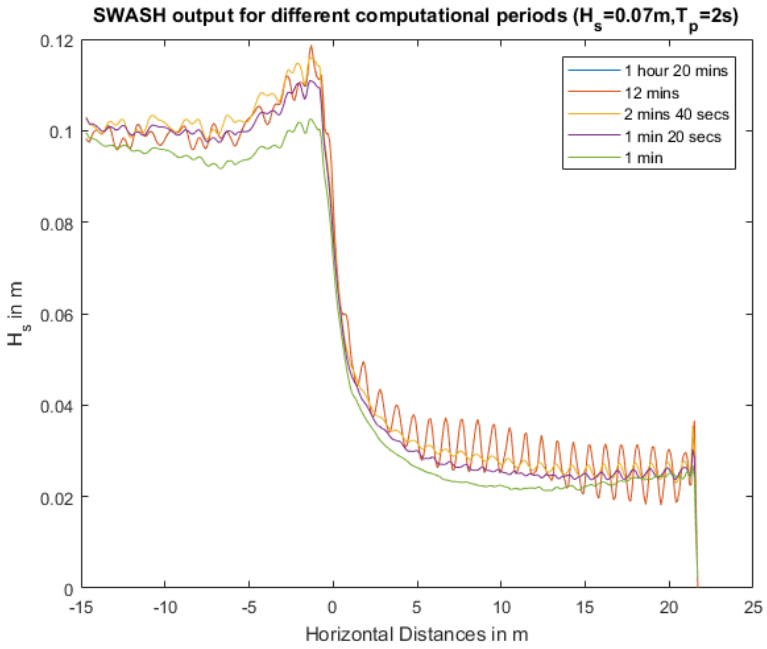

Figure 3.7: SWASH output for Regular Wave case with different computational period

[12] That is, the first 150 waves (each having a T of 2 s) were sacrificed.

In general, the shape of the output agrees with the theory; breaking occurs where the waves become depth-limited. Around the foreshore tip (‘0’ on the x-axis), it is also marked that the wave heights increase. In the foreshore region, a very regular pattern of undulation is observed.

3.5.4.2. Bichromatic Case

Figure 3.8 shows the output of the bichromatic wave input, along with the regular wave input, the runtime being 1 hour and 20 mins. It is observed that the wave heights are comparatively much higher in the bichromatic wave case than the regular wave case. Furthermore, there is a pattern of the wave heights observed in the foreshore region.

Figure 3.8: SWASH output for two wave cases

3.6. Comparison of the Models

When the outputs of both the models are compared side-by-side, the results get clearer. Figure 3.9 shows the outputs of the regular wave case, as given by the two models, SWAN and SWASH.

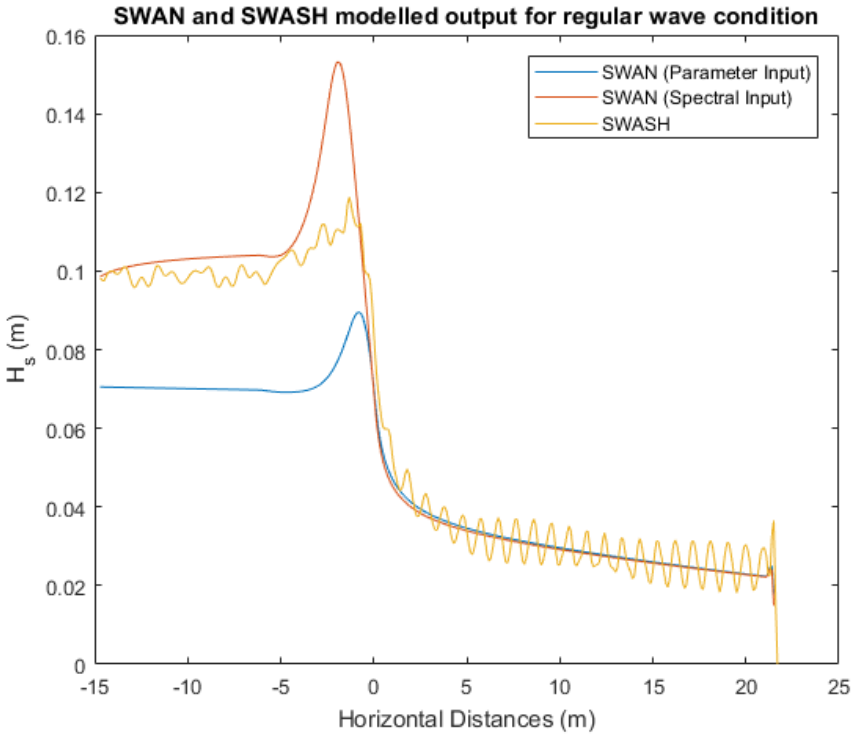

Figure 3.9: SWAN and SWASH output for regular wave condition

As seen, the overall shapes agree with each other. The nearshore processes are also observed. There is shoaling as the waves approach the coastline. As explained in Appendix C, the input spectrum for the SWAN run is obtained from the surface elevation at the offshore-most location. This process is seen in Figure 3.9 as well as in Figure 3.10, i.e., the output at the said location is the same.

Figure 3.10 shows a similar comparison in case of bichromatic waves. One thing stands out is that the wave heights are overall higher in SWASH output than in SWAN.

As the waves progress, they steepen. As soon as the waves reach the depth for breaking, they break, and the wave heights instantly fall. Then on, in the foreshore region, regular undulations in the SWASH graph is seen. It is also noted that the SWAN output in the foreshore region is approximately the mean of the SWASH outputs. We also see that the wave run-up estimations of SWASH are higher than that of SWAN.

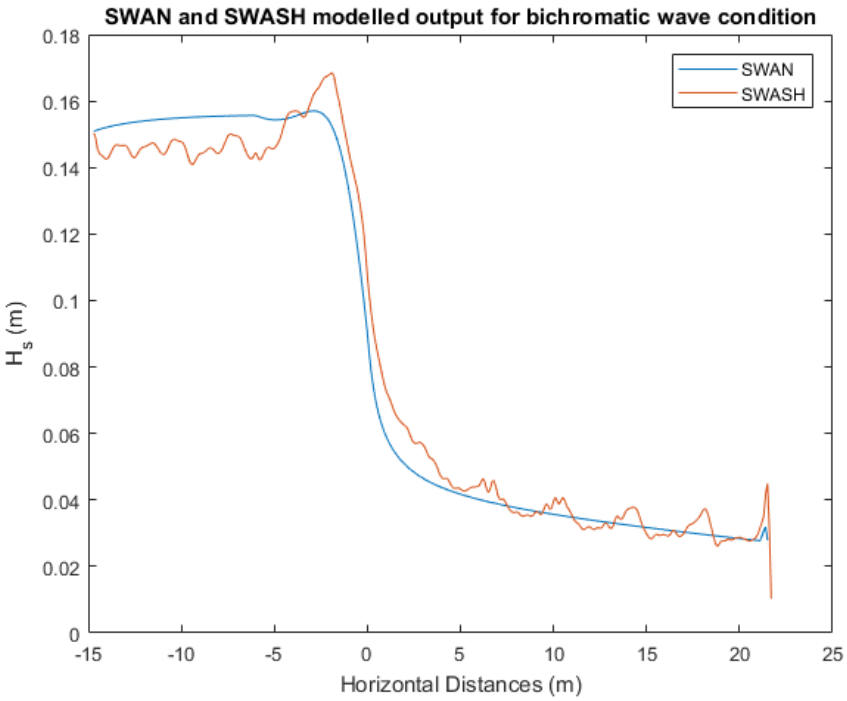

Figure 3.10: SWAN and SWASH output for bichromatic wave condition

Of course, the approach to the problem is different in different models, as the underlying principles and calculation methods are different. However, the overall shape agreeing and the theoretical processes being reflected in the output is a good indicator of the acceptability of the models. The models are further tested in the next chapter along with the measured data from the laboratory.

4
VALIDATION

To measure is to know.
William Thomson Kelvin

This chapter first introduces the laboratory data that was collected and the associated data processing. Then, the SWAN and the SWASH models' results are presented, and a comparison was made of the estimated results keeping the observed data in mind.

4.1. Laboratory Data

4.1.1. Bathymetry

As mentioned in Chapter 3, a laboratory condition was set up in the TU Delft Laboratory of Fluid Mechanics flume. This condition reflected a typical shallow foreshore in the tropics. The schematized profile is shown in Figure 4.1. Even though the foreshore is flat, it can be considered a representation of the vegetated coasts, as those coasts have very gentle slopes over kilometres. As for the relatively steep part (from -6 m to -1 m) is present as such, because the flume is otherwise not long enough.

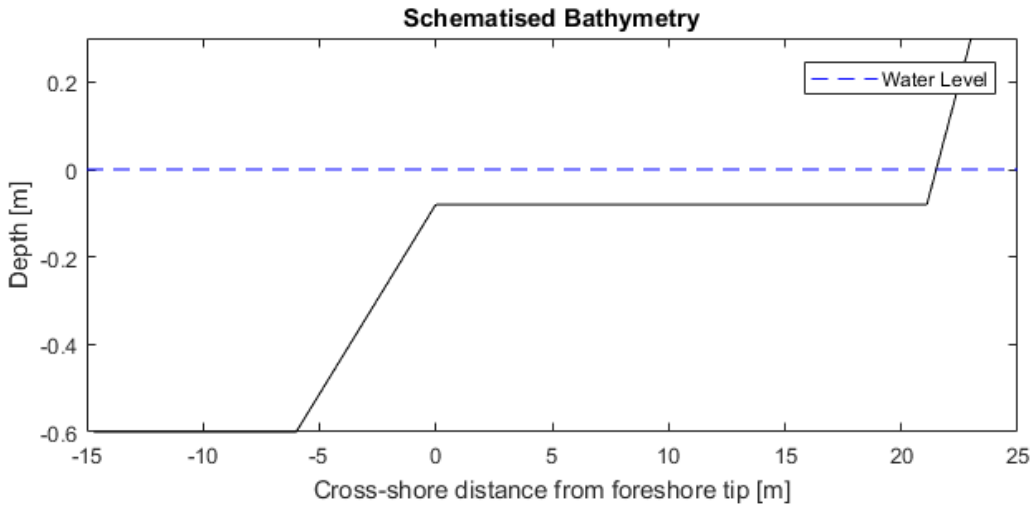

Figure 4.1: Schematized Bathymetry used in modelling

4.1.2. Input Parameters for Wavemaker

The wavemaker was run to make a bichromatic wave condition. The water depth at the wavemaker was 0.6 m, i.e., the offshore water depth.

Three cases were evaluated, as follows:

Case 1
Wave Heights of $H_1 = H_2 = 6$ cm, Wave Periods of $T_1 = 1.67$ s and $T_2 = 2.5$ s.

Case 2
Wave Heights of $H_1 = H_2 = 8$ cm, Wave Periods of $T_1 = 1.39$ s and $T_2 = 1.62$ s.

Case 3
Wave Heights of $H_1 = H_2 = 8$ cm, Wave Periods of $T_1 = 1.82$ s and $T_2 = 2.24$ s.

Each case was checked separately.

4.1.3. Wave Gauge Data

The wave gauges were installed at -9 m, -1 m, 5 m, 7.5 m, 10 m, 12.5 m, 15 m, 17.5 m, and 21 m. They were not installed further offshore to prevent any data disruptions due to the wavemaker itself and also, it was not necessary as such because the waves were not expected to transform much in very deep waters. They were first calibrated to the lab condition, giving a multiplication factor of 0.025 to convert the voltage signal (in V) to surface elevation (in m). The data obtained from the wave gauges were converted accordingly to the surface elevation signal. A residual signal was present in the wave gauge which was removed from the total signal. Then, a clean signal is obtained.

4.1.3.1. Surface Elevation – Case 1

Figure 4.2 below shows the (clean) surface elevation signal, as measured at -9 m. It shows a short time lapse from 1490 s to 1530 s, i.e. 40 seconds from 1490 seconds after the start of the measurement[13]. It shows quite a regular pattern of the surface elevation that is expected. The upper and lower limits are also as anticipated, at around ±0.06 m. This value is the wave group amplitude. Thus, the wave group height is around 0.12 m, which is by linear superposition theory obtained from adding the individual components' wave heights.

As the waves progress along the flume, they start transforming and breaking, as per theory. These processes are also seen in Figure 4.3 (left), showing the surface elevation record at -1 m, in the breaker zone, and at 21 m (Figure 4.3 - right), in the swash zone. Signals are quite as expected. At -1 m, it gets depth limited, and at 21 m, it becomes irregular.

[13] No specific reason for why the author chose this particular time lapse period. This was just to show the regular surface elevation pattern after being stabilised after running the wavemaker/model for around 25 minutes (1500 seconds).

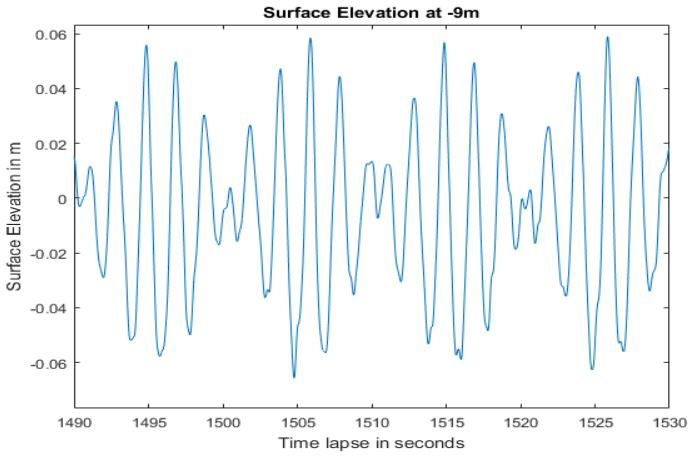

Figure 4.2: Surface elevation at -9 m for a short time lapse (Case 1)

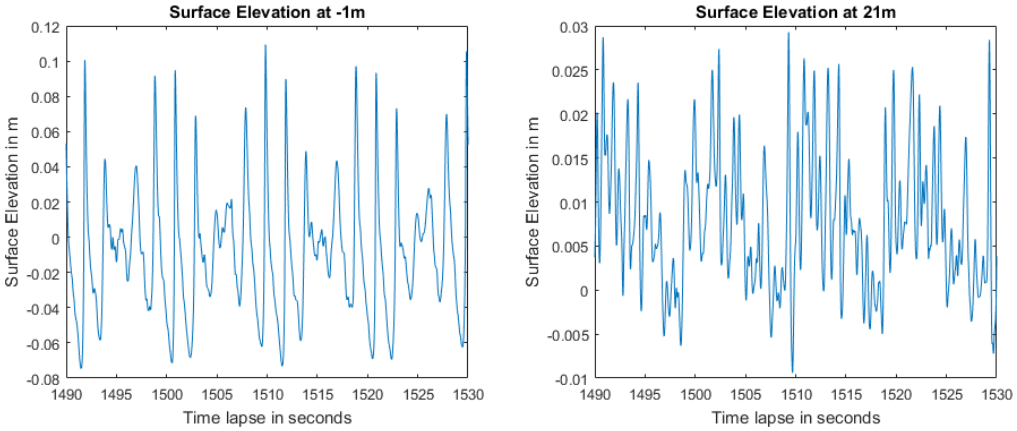

Figure 4.3: Surface Elevations at -1 m and 21 m (Case 1)

4.1.3.2. Surface Elevation – Cases 2 and 3

Figure 4.4 shows the surface elevation record at the same location (-9 m) for Case 2 and Case 3 conditions. The upper and lower limits are as expected (±0.08 m).

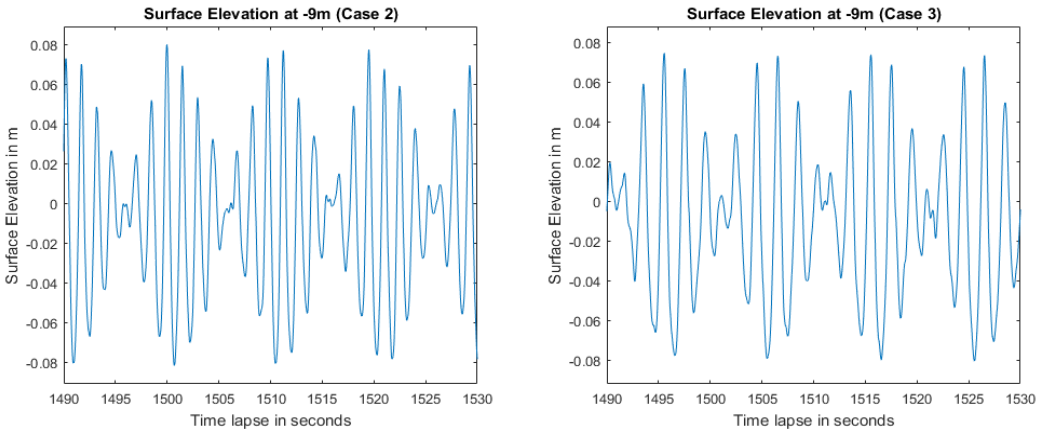

Figure 4.4: Surface Elevations at -9 m (Cases 2 and 3)

4.1.4. Spectral Analysis of the Data

A spectral analysis of the data was done to understand the surface elevation record better. Ultimately, this step is also necessary if one has to use the SWAN model, which is a spectral model and needs a spectral input.

4.1.4.1. Choice of Number of Blocks

To do a spectral analysis, a selection of the number of blocks, to divide the data into, must be made. If we, let's say, do not split the data at all, the spectrum so obtained will be a 'raw' estimate, with an error having an order of 100% because the variance density was estimated from only one amplitude per frequency. Figure 4.5 shows the 90% confidence limits[14] and frequency resolution with respect to the number of blocks. As we can see, as the number of blocks increases, the confidence increases, i.e., the limits' coefficients nearly coincide and is around 1, thus the accuracy of the predictions is very high. The disadvantage of increasing the number of blocks, however, is that the resolution is gradually lost. On balance, 36 is chosen as the number of blocks to go forward with.

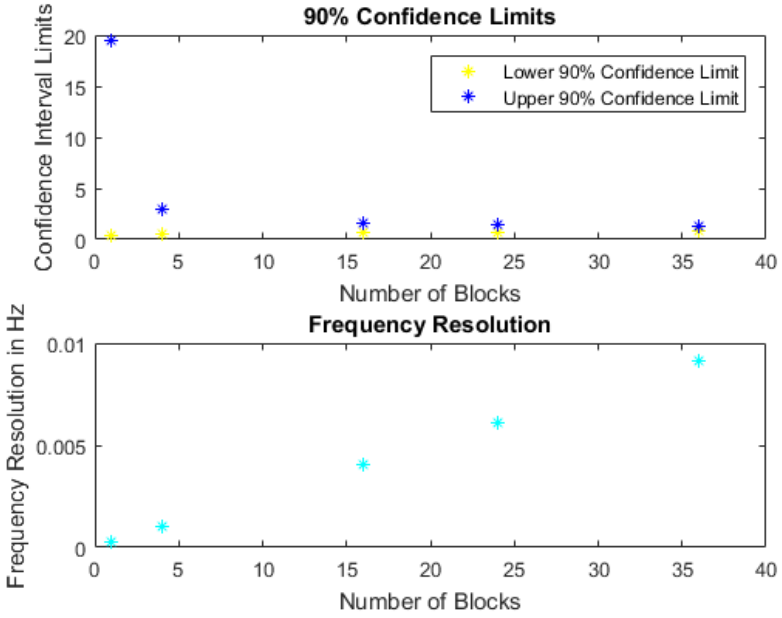

Figure 4.5: Confidence Limits and Frequency Resolution versus number of blocks

4.1.4.2. Variance Density Spectrum – Case 1

After doing a spectral analysis of the surface elevation record at -9 m for Case 1, the resulting variance density spectrum record was obtained, that is shown in Figure 4.6. The record shows a presence of Very Low Frequencies (VLF), i.e., the frequencies below 0.01 Hz. This presence was also observed by Bakker (2017) in her (purely theoretical input) runs with the SWASH model. In nature, waves with such low frequencies do not exist. The presence of this in the laboratory might be due to various reasons. One reason can be because of the wave reflections from the landward boundary of the flume.

[14] 90% confidence limits mean that we have a 90% confidence that the data lies within the lower and upper limits. This is expressed as a coefficient that should be multiplied to the actual data to show the range that the data might lie in.

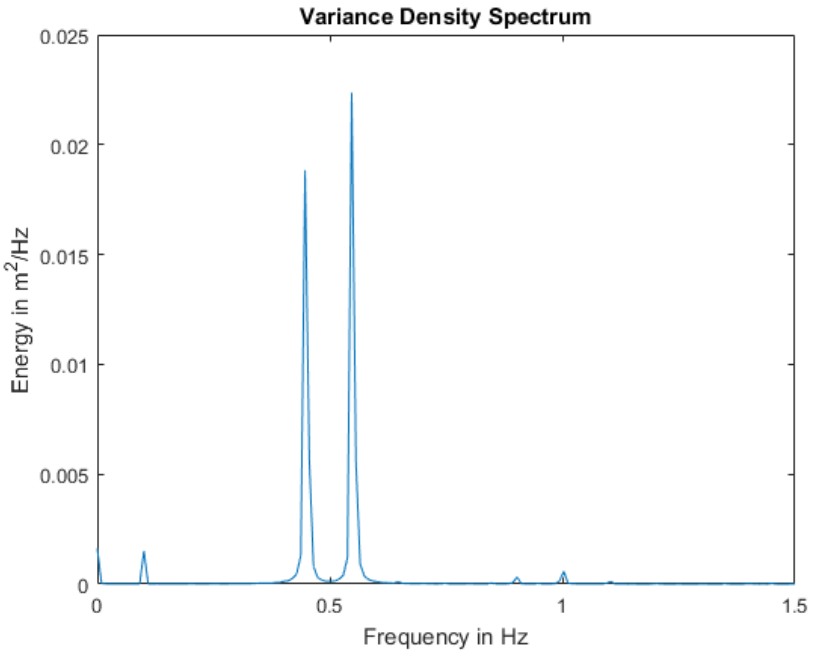

Figure 4.6: Variance Density Spectrum for elevation record at -9 m (Case 1)

4.1.4.3. Variance Density Spectrum – Cases 2 and 3

Figure 4.7 shows the variance density spectrum records at the same location (-9 m) for Case 2 and Case 3 conditions. These records also demonstrate the presence of VLFs and other higher frequencies.

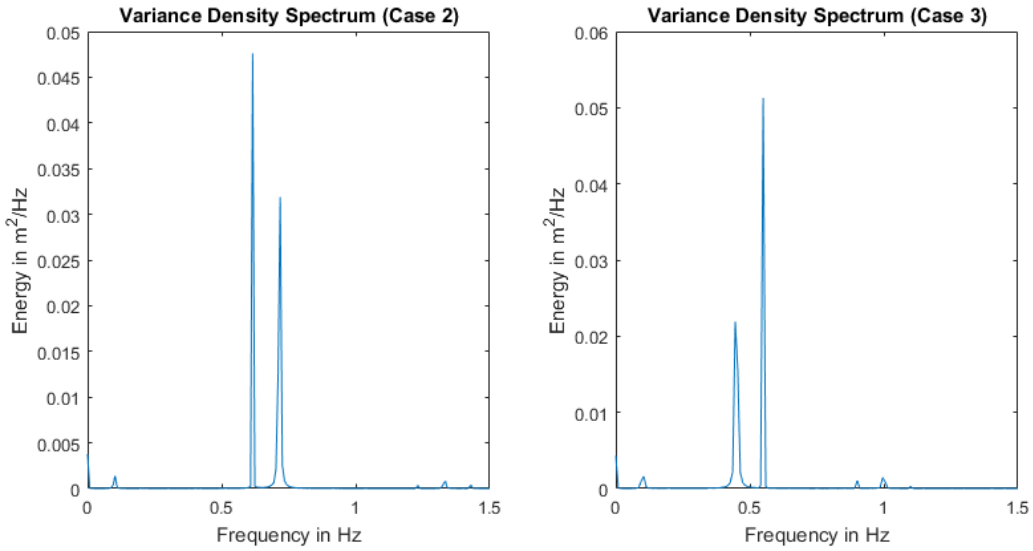

Figure 4.7: Variance Density Spectrum for elevation record at -9 m (Cases 2 and 3)

4.1.4.4. Variance Density Spectrum - Filtering

For the model runs, these spectrum records are useful. These records were also filtered, i.e., the small energy peaks were removed without compensating them into the main energy peaks, to see how these frequencies affect the output. Figure 4.8 shows the filtered surface elevation of Case 1 and Figure 4.9 shows the filtered spectrum of Case 1. One

can see the differences by comparing these figures with Figure 4.2 and Figure 4.6 respectively. Similar filtering was done for Cases 2 and 3.

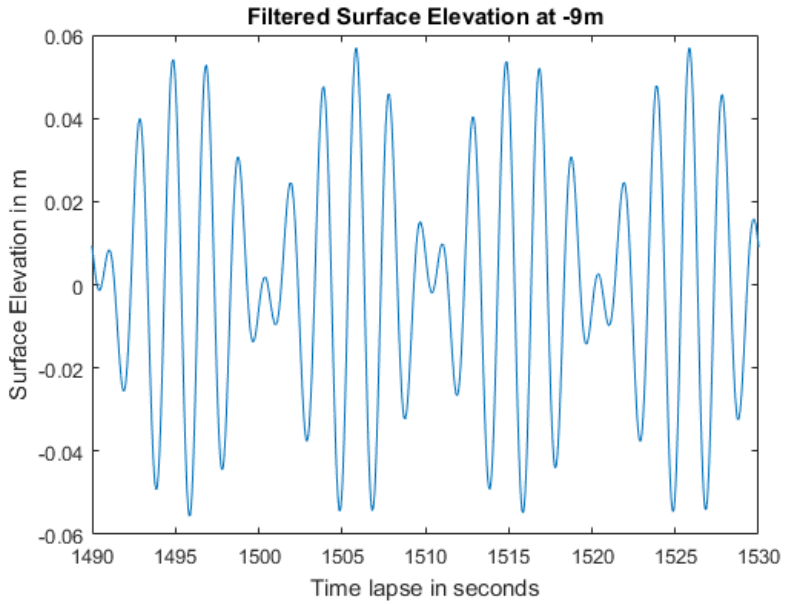

Figure 4.8: Filtered Surface Elevation at -9 m (Case 1)

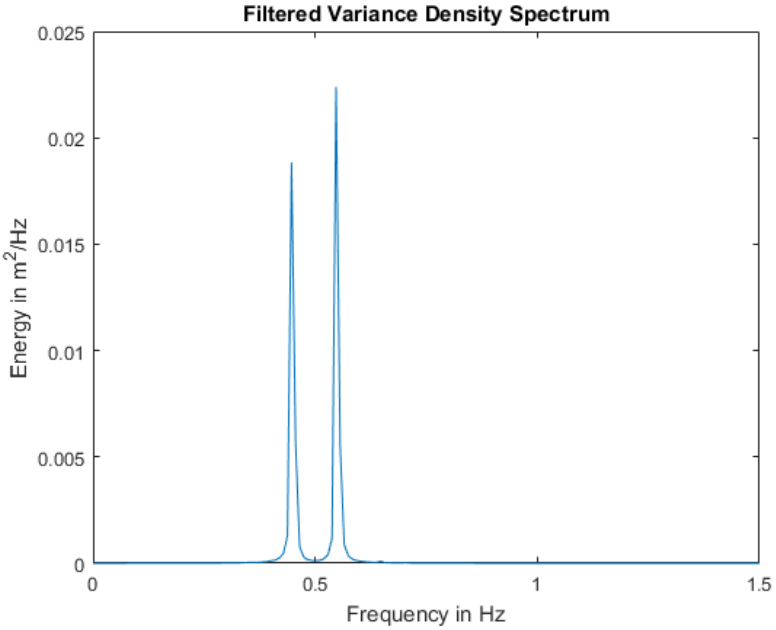

Figure 4.9: Filtered Variance Density Spectrum (Case 1)

4.1.5. Significant Wave Heights from the Wave Gauges

As explained in Equation (3), the significant wave height is the mean of the highest one-third of waves in the wave record. The surface elevation record, for each wave gauge location in the foreshore region, was analysed to obtain the number of waves (using the downward zero-crossings approach) and wave heights and subsequently the significant

wave height values[15] at those locations. This analysis was done for all the three runs of the wavemaker. The results are shown later along with the outputs of the models.

4.2. SWAN

4.2.1. Model Inputs

As mentioned earlier; SWAN is a spectral model. This means that for input, it cannot accept surface elevation inputs, nor does it give such outputs. To use the lab data as an input, it had to be converted to a spectrum record. Three sets of conditions were used as input for the SWAN model in each of the three cases:

- Spectrum input, as it is obtained from the surface elevation record.
- A corresponding filtered spectrum input of the above.
- Bichromatic wave input, replicating the initial wavemaker input conditions.

The procedure as explained in Appendix C is used to obtain a spectrum to be used in SWAN.

4.2.2. Model Outputs

4.2.2.1. Case 1

Figure 4.10 shows the modelled wave heights as per the three sets of conditions. As can be observed, in the surface elevation - spectrum input case, the initial value is 0.1 m, while the surface elevation signal has a group wave height of 0.12 m. The filtering of the elevation record has reduced the initial wave height. After breaking, however, the wave heights are the same.

For the theoretical spectrum input, the starting wave heights are higher, but around the theoretical group wave height of 0.12 m. The reason for the decrease of the wave heights might be because of how SWAN treats the spectrum. The wave heights decrease between the start of the propagation at -14.7 m and at the wave gauge measurement location at -9m. One of the plausible reasons might be a slight loss of energy between -14.7 m and -9 m for various of physical reasons, resulting in this decrease of wave heights.

In the foreshore region, however, the theoretical bichromatic wave spectrum input gives slightly higher wave heights. Figure 4.10 also shows the significant wave height values, as measured in those locations in the laboratory. It seems that SWAN does not reflect this pattern at all, but just giving an output of an average wave height along the foreshore.

[15] Since, as mentioned earlier, the models give H_s values as output, it obviously makes sense to compare H_s to H_s.

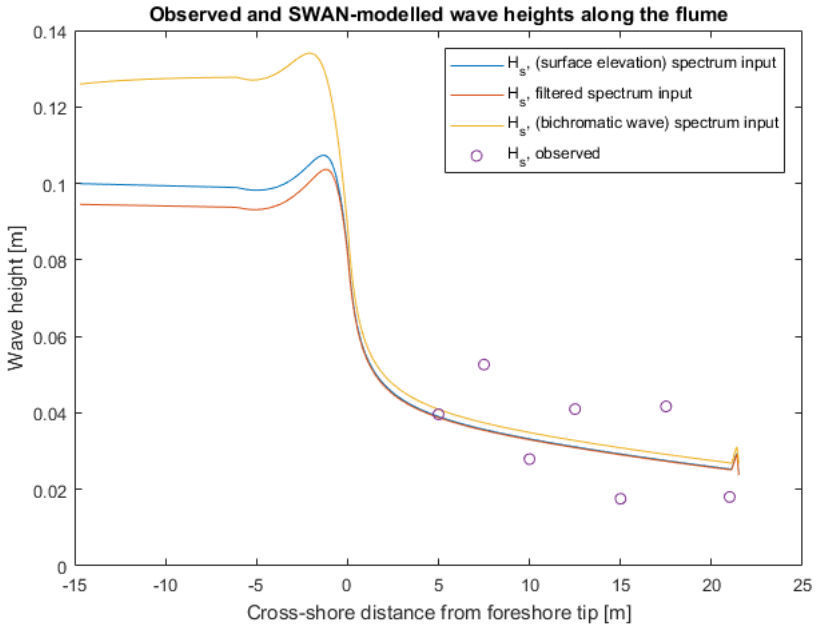

Figure 4.10: SWAN-modelled wave heights along the flume (Case 1)

4.2.2.2. Case 2

The results of the Case 2 input are shown in Figure 4.11. In this case, filtering results in slightly decreased wave heights. Also, the wave heights for the theoretical input is higher than the supposed wave height of 0.16 m. The graph of this case, however, is a bit different than what is observed in Case 1. The wave heights just decrease, with no marked sign of shoaling.

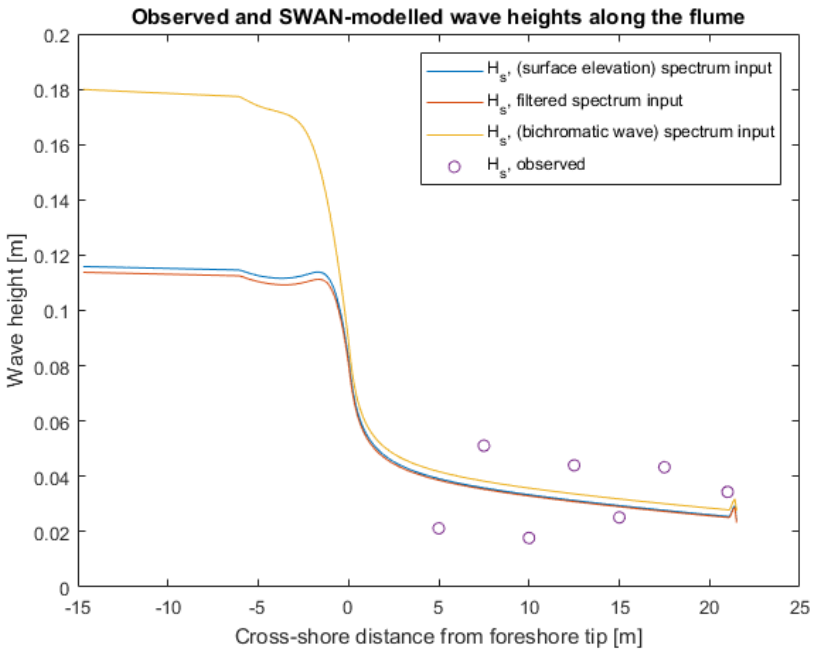

Figure 4.11: SWAN-modelled wave heights along the flume (Case 2)

4.2.2.3. Case 3

Similarly, Figure 4.12 shows the results for Case 3 conditions. The only difference between the inputs of Case 2 and 3 are the wave periods (reference is made to Section 4.1.2). As seen in Figure 4.12, the wave heights at the offshore location are slightly higher. Filtering in Case 3 results in a considerable change in the offshore wave heights, without any changes after wave breaking. Also, in the theoretical spectrum input, the shape of the graph is different.

These results show that keeping the wave height constant and changing the wave period leads to a change in offshore wave heights, as well as a change in the overall SWAN-modelled shape of the graph (in the bichromatic wave input condition).

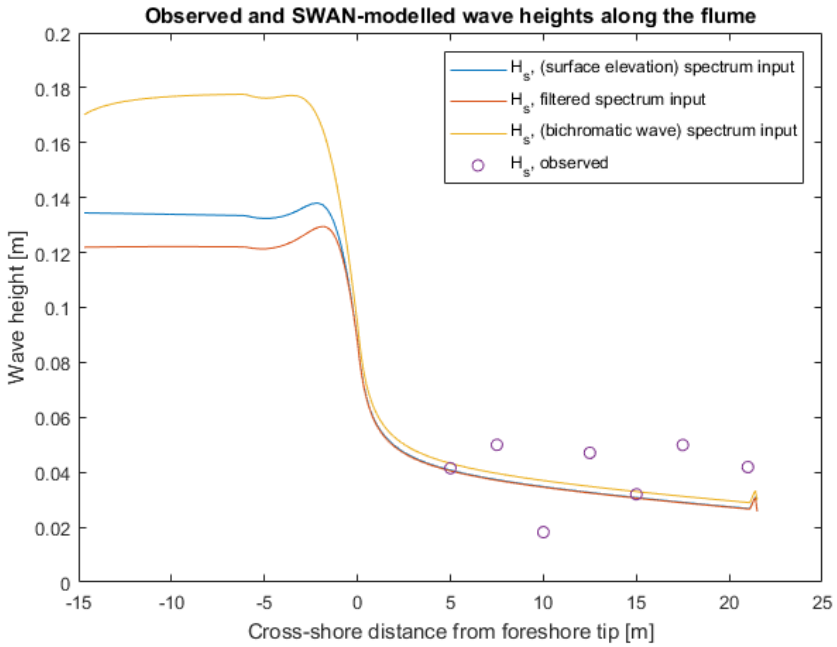

Figure 4.12: SWAN-modelled wave heights along the flume (Case 3)

4.3. SWASH

4.3.1. Model Inputs and Set-up

As mentioned earlier; SWASH is a time-domain model. This means that it accepts a time series input (surface elevation input), and also can give such an output. A spectrum can also be used as an input, and SWASH generates a time series from the spectrum, as per linear wave theory. However, it is always better to input a time series, if available (M. Zijlema, personal communication, May 2017). Thus, the lab data was used as-is as an input (first condition). Three sets of conditions were used as input for the SWASH model in each of the three cases:

- The surface elevation record, as obtained from the wave gauge at -9m.
- A filtered elevation record of the above record.
- A bichromatic wave in the form of a Fourier series input, replicating the initial wavemaker input conditions.

The spin-up time in these runs was 20 minutes (i.e., the first 120 waves, with a group period of 10 seconds, were sacrificed).

4.3.2. Model Outputs

4.3.2.1. Case 1

Figure 4.13 shows the modelled wave heights as per the three sets of conditions. As seen in the figure, the original surface elevation results in higher wave heights in the offshore region. The reason for the increase in the wave heights might be because of how SWASH treats the time series. Also, the wave heights might have increased between the start of the propagation at -14.7 m and at the wave gauge measurement location at -9 m. As mentioned before, this can be because of the wave reflections from the landward boundary.

Filtering results in a slight decrease in the wave heights in the offshore region. One thing to note is that the wave heights increase very rapidly after the first point.

In the foreshore region, the difference is quite noticeable. Filtering makes the signal purely bichromatic, without any other waves present. When the filtered output and the original signal output is compared, it is seen that purifying the signal results in pronounced undulations seen in the foreshore part. Also, the overall wave heights are higher.

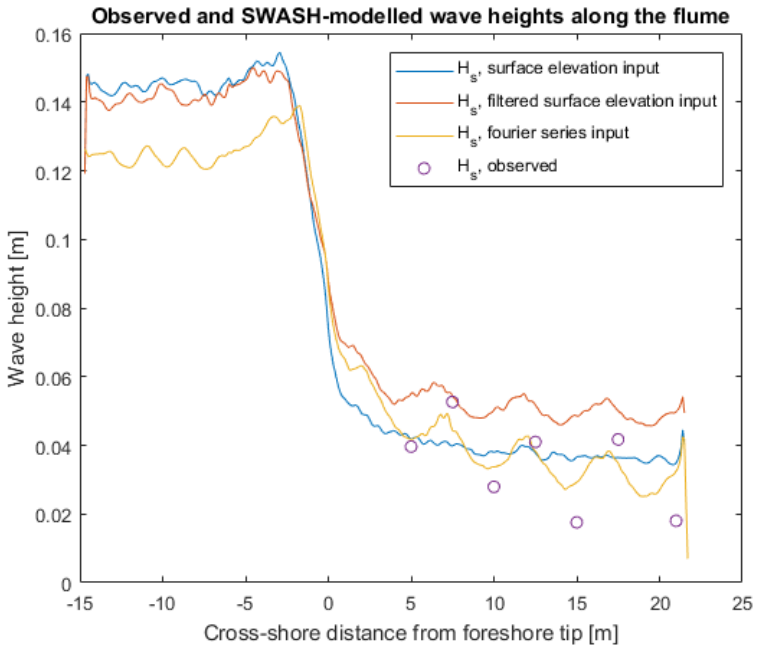

Figure 4.13: SWASH-modelled wave heights along the flume (Case 1)

When the Fourier bichromatic wave input was used, the wave heights are lower in the offshore region, but the starting value is as wished (at around 0.12 m). The foreshore results also reflect the undulation pattern seen in the filtered case.

When the observed wave heights are compared with all the conditions, the Fourier input seems to correlate the pattern the most of all the cases. This is a good sign, as in real life, one will just have some parameters to put into the model rather than measured data.

4.3.2.2. Case 2

Figure 4.14, similarly, shows the results for the three input conditions of Case 2. Overall observations are as seen for Case 1. The only small differences are that in the offshore region, the wave patterns for filtered and Fourier input have similar output shapes, and in the foreshore region, the filtered input has smoother fluctuations in comparison to the Fourier input. The Fourier input better reflects the observed pattern than other inputs.

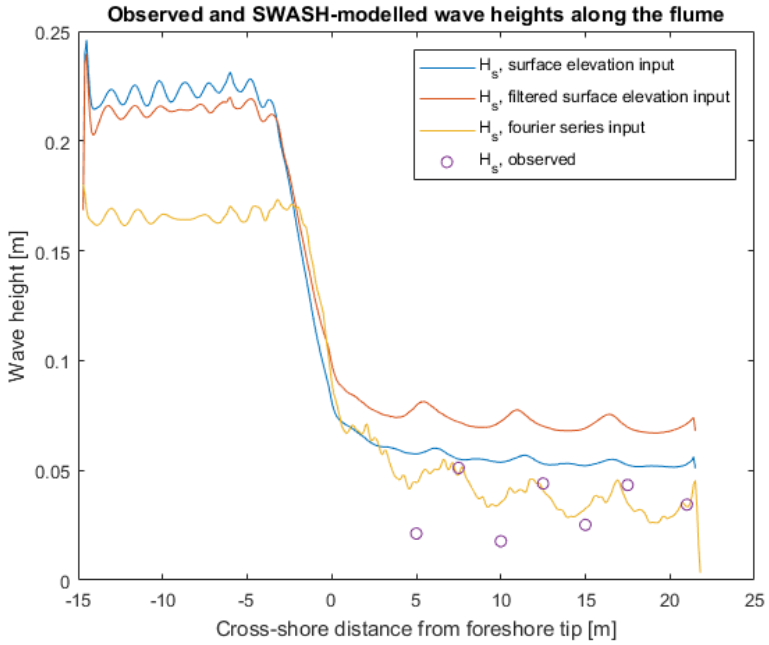

Figure 4.14: SWASH-modelled wave heights along the flume (Case 2)

4.3.2.3. Case 3

Similar to the other cases, Figure 4.15 shows the results for Case 3. No idiosyncrasies are present as such. The patterns in the outputs in the offshore region do not match with the filtered outputs, unlike in Case 2. The difference here is that there is a regular pattern observed in SWASH predictions in the offshore region in Case 2 rather than in Case 3. Also, the sudden wave height increase seen in Case 2 is not present in Case 3 (for surface elevation input). This differences can only be due to the changed wave period, thus the frequencies. Hence, it also somewhat shows that the change of frequencies and their interaction affect the outputs in the offshore region, just like in the foreshore region.

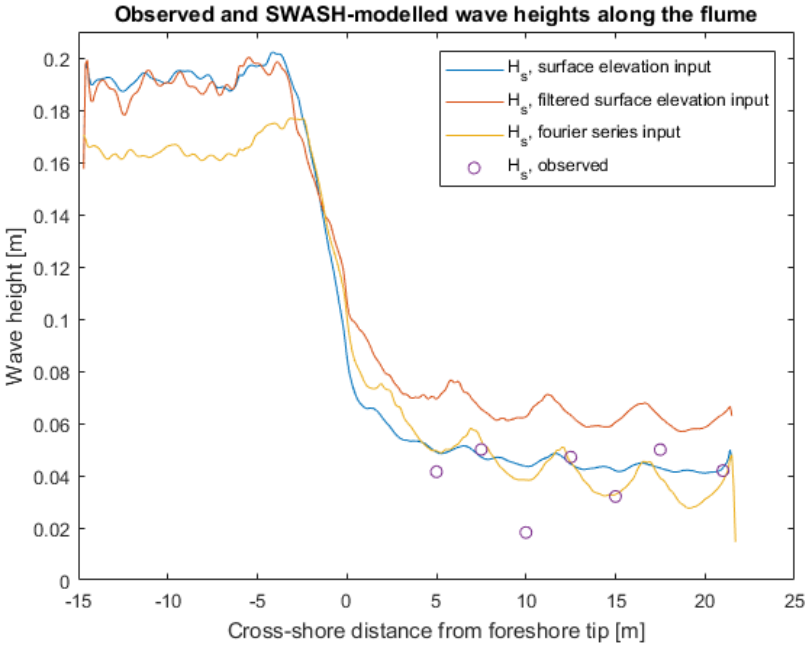

Figure 4.15: SWASH-modelled wave heights along the flume (Case 3)

4.4. Comparison of the Models

For comparison of the models, the theoretical inputs were used as an indicator, because in the absence of any laboratory (and by extension, field) data, which is usually the case in common situations, these inputs can show the overall performance of the models.

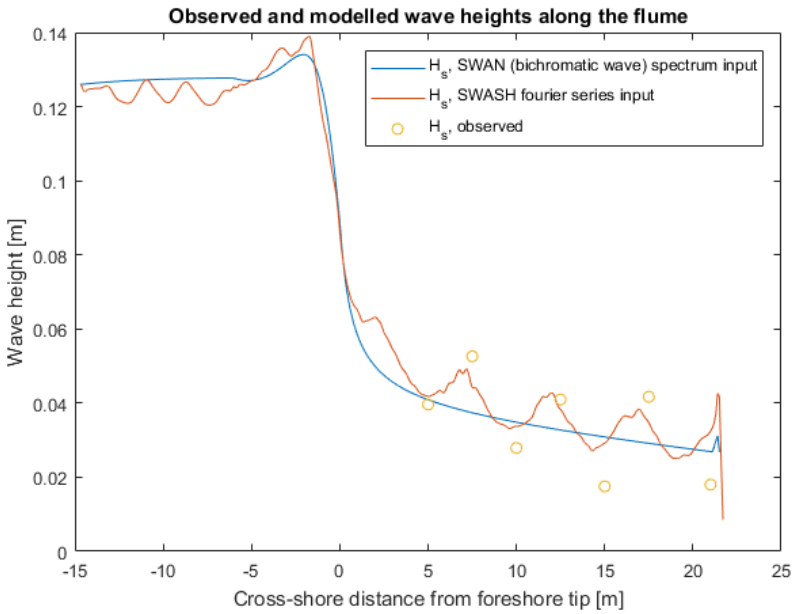

Figure 4.16: Modelled wave heights for the theoretical input (Case 1)

Figure 4.16 shows the SWAN (with a spectral input) and SWASH (with a Fourier parametric input) outputs for Case 1 theoretical condition. As observed, the overall shapes match a lot. Even the first value at the offshore is the same, before diverging. SWASH shows fluctuations everywhere, while SWAN does not.

In the foreshore region, the result is the same. SWAN does not replicate the bichromatic undulations, as seen in SWASH.

On comparing in the foreshore region, SWASH prediction follows what is observed in the laboratory. On the first glance, already, one can say that SWASH gives a better prediction in the foreshore region.

If the swash zone is inspected (i.e., roughly around 21 m), SWAN predicts a run-up, but it significantly lower than what SWASH predicts. We can also say that SWAN is underestimating the expected values. This underestimation is not good when we are interested in designing a coastal defence structure at the shoreline and want to use a model to predict the values, and the model underestimates these values.

Figure 4.17 and Figure 4.18 show similar comparisons for Case 2 and Case 3 respectively. In general, the comparison leads to similar observations as was from Figure 4.16. One thing that was common in all the cases was that in the offshore region, SWAN wave height predictions are higher than the SWASH predictions.

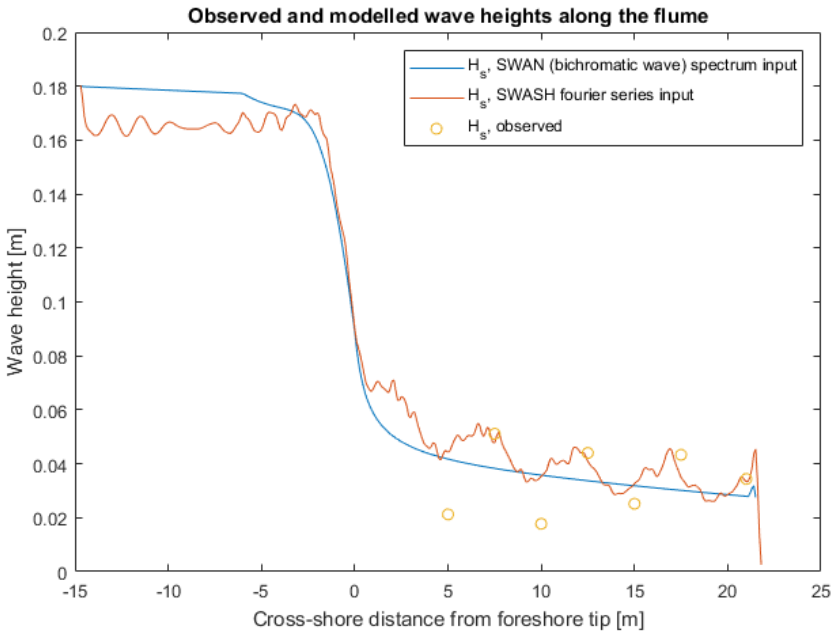

Figure 4.17: Modelled wave heights for the theoretical input (Case 2)

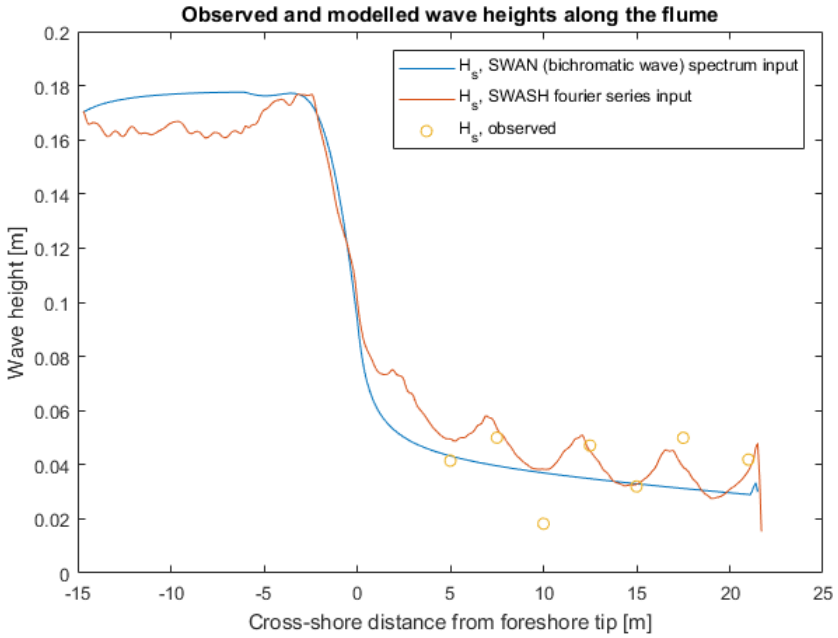

Figure 4.18: Modelled wave heights for the theoretical input (Case 3)

5
CONCLUSIONS

The best way to predict the future is to create it.
Abraham Lincoln

In this final chapter, a brief discussion and a summary of the relevant conclusions and recommendations are presented. This discussion is necessary to paint a bigger picture of the research and its further applicability.

5.1. Discussion

From the earlier research done, it was known that vegetation, such as mangroves, help in wave attenuation. It was also known that various numerical models predict the wave behaviour in the coasts. However, how these models predict the wave behaviour on coasts with shallow foreshores is somewhat unclear. The main research question that was proposed in Chapter 1 as:

> ***How can we, to a certain degree of accuracy, determine how the waves behave and transform at a coast, that is typically vegetated?***

This thesis first started with a brief theory of the waves and their transformation in oceanic and coastal waters. Then, the models used in this research were introduced, and some initial tests were done, with regular and bichromatic waves. Then on, validation tests were done, for bichromatic waves for both the models, where the correlation between model predictions and the observed data was checked.

To start making conclusions, it is necessary to look back once and have a brief discussion on the sub-questions that were proposed initially.

1. *How do waves behave on a foreshore, that is generally found on tropical vegetated coastlines?*

   As known from background literature, waves propagate from deep waters into shallow waters. As they do so, they start feeling the bottom, i.e., they start to evolve and transform. The propagation first follows linear wave theory and then many nonlinear processes start occurring, such as shoaling, refraction, and diffraction. As seen in the measured data for the bichromatic wave, an oscillating pattern is noticed.

2. *What is the necessity of the used models?*

Models are essentially used to predict various things. They are nowadays used in basically every field of science and engineering, and beyond. In this study, two models are used, namely SWAN and SWASH. Both are developed at the Delft University of Technology to offer two different approaches to the same problem, one being a wave averaged (phase-averaged) model and the other being a short-wave resolving (phase-resolving) model. We wanted an answer to the wave predictions on the shallow foreshores, and thus it was a good idea to see and compare predictions from these models.

3. *How do the models behave on theoretical conditions?*

As seen in Chapter 3, the overall behaviour of the models was as expected and as per our knowledge in theory. The predicted values of the models differed in both the offshore and foreshore portions of the bathymetric profile. In the offshore region, the variations were based on how the model handled the input conditions. The variations were more noticeable in the foreshore region, in particular for a bichromatic wave. SWAN more or less averages the wave height values in the foreshore for both the regular and bichromatic waves. SWASH does not do this averaging, and it predicts otherwise. This perhaps is not so important when there are regular waves, but it is critical when bichromatic waves are considered because the wave height patterns are not adequately reflected in SWAN. SWASH predicts the wave height patterns which probably is caused when the two constituent components of the bichromatic wave are either in-phase or out-of-phase at various locations along the foreshore length in the cross-shore direction.

4. *How do the results obtained from laboratory tests match up with the predicted model results?*

As seen in Chapter 4, when the models were inputted with the laboratory data, in the form of either measured or filtered surface elevation data (for SWASH), and the corresponding spectra (for SWAN), the overall predictions of the models were consistent with what the theoretical observations were. The measured laboratory observations did not quite match up with the data. Reasons that can be thought of are that for SWAN, it is because of the wave-averaging approach, and for SWASH, it is the higher wave heights that are put as the boundary condition, leading to higher wave height values in the foreshore. For SWASH (in the filtered state), the wave height patterns match with the overall shape of the observed wave heights along the flume.

5. *Conversely, how do the models predict the results when inputted with the laboratory conditions?*

When the models were inputted with the parameters that created the waves in the wavemaker, the predictions in SWAN more or less remained the same as in the laboratory spectrum input cases. In SWASH, however, the overall predictions matched up quite well with the observed data.

5.2. Conclusions

The conclusions that have been drawn from this research are explained below.

5.2.1. Offshore Region

- Variation of input conditions leads to changes in the predicted results, as expected.
- Varying the same wave condition by the form it is inputted in (parametric or spectral), changes the offshore predictions in SWAN due to the way it interprets the input.
- Changing the spectral distribution changes the offshore predictions in SWAN. The runs with a sectoral grid spread are computationally expensive than a circular grid spread.
- Changing the computational run-time slightly changes the offshore predictions in SWASH.

5.2.2. Foreshore Region

- The foreshore predictions in SWAN changes with a change in wave type but does not change with a change in the kind of input of a specific wave condition.
- In general, for SWAN, **what happens in the offshore region do not affect what goes on in the foreshore region**. There is some kind of memory loss, so to say.
- The foreshore predictions in SWASH in the regular wave changes with the computational period. Hence, it is essential to run the model for a sufficient duration to be able to obtain reliable predictions.
- **SWASH correctly predicts the wave height variations**, in both the wave conditions and proved by comparing with the measured data in the laboratory. This corroborates one of the recommendations made by Janssen (2016), i.e., to use a phase-resolving model for flood risk assessments, for instance, especially in a shallow foreshore coast that is vegetated.
- **SWAN underestimates the wave heights**. This becomes necessary, especially in bichromatic wave case, when the in-phase interaction of the components, resulting in the maximum wave heights, are underpredicted. This underestimation will have a serious consequence when trying to estimate run-up and overtopping volumes, which are essential parameters for designs of coastal defence structures.
- As observed from the predictions, differences in the offshore region do not affect how the models behave in the foreshore region. Thus, the specific conclusions above are valid.
- A strange thing that was observed that filtering the elevation data makes the undulating wave height patterns more pronounced. This is contrary to what we know from literature. van Gent (2001) reasons that the wave run-up will be governed by the low-frequency wave motion than compared to the high-frequency motion.
- If we refer back to Table 2.1 and Figure 2.6, for instance, we see that the triad wave-wave interaction is a dominant process in the nearshore region. Moreover, the presence of VLF and higher frequencies (due to the triad interaction) will make the undulations more pronounced. However, their removal led to more pronounced undulations. Reason can be thought of is that the various frequencies counteract

each other's effects, leading to milder undulations. When the VLFs and higher frequencies are removed, the two largest components interact amongst each other only, resulting in the higher and lower wave heights when the components are in-phase (constructive interference) and out-of-phase (destructive interference) respectively. The interference was expected because the bichromatic wave components have the same amplitude and propagation direction. This proposition is also backed by the similar SWASH results for the laboratory condition-replicating theoretical (i.e., pure two-peaked spectrum) conditions.

- However, the presence of these other frequencies was initially assumed as due to the wave reflections from the landward boundary. So, if this indeed is the case in real life, it will be advantageous, since it will lead to lowering of the maximum wave heights hitting the coastal defence structure.

5.2.3. Advances

This study tried to bring more clarity into the model predictions and how applicable they are, when checked with measurements, especially in the foreshore region. As observed, we have some answers, and further research can be based on these results. We saw an interesting anomaly, and this definitely needs further investigation.

This study marks a step towards answering the main research question and starting to understand the "wave transformations on shallow foreshores" more, as the title of this thesis states.

5.3. Limitations

This study was limited by two main factors: consideration of only the hydrodynamics, and the simplifications made to simulate the conditions. In real life, even if we had field measurements, a lot of additional factors would have been automatically added, the main factor is the inclusion of vegetation, and the added uncertainties, for instance, the presence and effect of sediments.

SWAN was run in stationary mode. If it was run in a non-stationary mode with the same time conditions as in SWASH, the results might be different (i.e., similar to SWASH results). Due to time constraints, this could not be tested by the author.

Another limitation can be the use of a model to model something, i.e., use of SWASH to obtain the inputs for SWAN's use. A brief comparison was done and is presented in Appendix D. It seems that the effect is not much, but this was not tested for the validation cases, but only for benchmark tests.

After all, some assumptions should be made, as no method is perfect and not all aspects can be included in the adopted method.

Key limiting model assumptions included:

- Idealised 1D profile consisting of a horizontal foreshore
- Non-inclusion of wind, i.e., the energy input from the wind was not considered.
- Single-peaked JONSWAP spectra
- Wind waves not considered
- Use of default values

- No 2D effects

5.4. Recommendations

Based on findings of the report, some recommendations are made on which further research can be based.

1. *Finding a transition point for the models, and using SWAN and SWASH together.*

   In the offshore region, as seen from the predictions, SWAN averages out the values. It is also observed that the changes happening offshore do not affect the wave heights foreshore. Moreover, since the variations offshore do not affect the foreshore values, SWAN can be used until some point and then on SWASH for further regions foreshore. One thing we know for sure is that SWASH predicts wave heights better in the foreshore region. We also know that SWASH does not include the wind-wave growth in the calculations (Tas, 2016). In a real-life scenario, it is better to include these in SWAN, which is much better in transforming and predicting waves from an offshore location to some point near the breaking point. This combined two-model use will result in a quicker assessment of the nearshore conditions and improve the computational efficiency of the overall project.

2. *Using other wave conditions to check the conclusions proposed*

   This study focused more on the bichromatic waves, which is a very theoretical condition, and how the models predicted wave heights for those conditions. However, it will be better to make similar comparisons for other conditions, for instance, with wind waves in addition to the bichromatic wave.

3. *Collect more field data*

   A scarcity of field data on which to validate the network is usually one of the key limitations in studies of this kind. Hence, additional data collection is essential for future work. Data from shallow foreshores near centres of high population density or critical infrastructure should be prioritised, as that is where we want to focus our study on, for the benefit of humankind.

BIBLIOGRAPHY

Bakker, S. A., 2017. *Coastal protection in the Mekong Delta,* M.Sc. Thesis: TU Delft.

Bosboom, J. & Stive, M. J. F., 2015. *Coastal Dynamics I.* 0.5 ed. Delft: Delft Academic Press.

Chella, M. A., Bihs, H., Myrhaug, D. & Muskulus, M., 2015. Breaking characteristics and geometric properties of spilling breakers over slopes. *Coastal Engineering,* Volume 95, pp. 4-19.

Dijkstra, J. T. & Uittenbogaard, R. E., 2010. Modeling the interaction between flow and highly flexible aquatic vegetation. *Water Resources Research,* Volume 46, pp. 1-14.

Giri, C. et al., 2011. Status and distribution of mangrove forests of the world using earth observation satellite data. *Global Ecology and Biogeography,* 20(1), pp. 154-159.

Harihar, S., 2015. *Design of Mangrove Rehabilitation Projects on Tropical Coasts,* M.Sc. Thesis: TU Delft.

Hasselmann, K. et al., 1973. Measurements of wind-wave growth and swell decay during the Joint North Sea Wave Project (JONSWAP). *Deutches Hydrographisches Institut.*

Holthuijsen, L. H., 2007. *Waves in Oceanic and Coastal Waters.* Cambridge: Cambridge University Press.

Janssen, M. P., 2016. *Flood Hazard Reduction by Mangroves,* M.Sc. Thesis: TU Delft.

Narayan, S., 2009. *The Effectiveness of Mangroves in Attenuating Cyclone-induced Waves,* M.Sc. Thesis: TU Delft.

NTNU, 2016. *TBA4265 Arctic and Marine Civil Engineering,* NTNU: Trondheim.

Phan, L. K., de Vries, J. S. M. v. T. & Stive, M. J. F., 2011. Coastal Mangrove Squeeze in the Mekong Delta. *Journal of Coastal Research,* 31(2), pp. 233-243.

Small, C. & Nicholls, R. J., 2003. A global analysis of human settlement in coastal zones. *Journal of Coastal Research,* 19(3), pp. 584-599.

Sutton-Grier, A. E., Wowk, K. & Bamford, H., 2015. Future of our coasts: The potential for natural and hybrid infrastructure to enhance the resilience of our coastal communities, economies and ecosystems. *Environmental Science & Policy,* Volume 51, pp. 137-148.

Suzuki, T. et al., 2011. Wave dissipation by vegetation with layer schematization in SWAN. *Coastal Engineering,* Volume 59, pp. 64-71.

Tang, J. et al., 2017. Numerical study of periodic long wave run-up on a rigid vegetation sloping beach. *Coastal Engineering,* Volume 121, pp. 158-166.

Tas, S. A. J., 2016. *Coastal Protection in the Mekong Delta,* M.Sc. Thesis: TU Delft.

The SWAN Team, 2016. *SWAN Scientific and Technical Documentation,* TU: Delft.

The SWAN Team, 2016. *SWAN User Manual,* TU: Delft.

The SWASH Team, 2017. *SWASH User Manual,* TU: Delft.

Tusinski, A., 2012. *The role of mangroves in the design of coastal dikes: Hydrodynamic and cost related aspects,* M.Sc. Thesis: TU Delft.

UNEP, 2017. *Global Clean Ports.* [Online]
Available at: http://staging.unep.org/transport/Ports/index.asp
[Accessed 15 05 2017].

van Gent, M., 2001. Wave Runup on Dikes with Shallow Foreshores. *Journal of Waterway, Port, Coastal, and Ocean Engineering,* 127(5), pp. 254-262.

A
SWAN SCRIPT

This appendix presents a brief overview of the SWAN script, otherwise known as the input code, as well as including a sample input file for each condition.

A.1. Benchmark Tests

A.1.1. Regular Wave

Start-up

The Nautical Convention was used for the wind and wave direction. This convention takes the direction the winds and waves are coming from. The water level was set at 0 because the lab condition is tide-free, but this can be changed based on the Mean Water Level (MWL) in a tidal situation. The maximum error level was set at 2, that is SWAN will not start computations if there are *errors* which are not automatically repaired by SWAN. Thus, *warnings* will not lead to stopping of the computation. SWAN is run in 1D mode (parallel depth contours) and Stationary Mode (non-time varying). However, refraction and directional spreading is included in the runs, but not diffraction. The threshold depth for computation was set to 0 m, instead of the default of 0.05 m, i.e., all the positive depths are considered as is, instead of the ones smaller than 0.05 m being changed to 0.05 m. In large scales, this threshold depth might not affect much, but in this laboratory scale, it might.

Computational Grid

The Computational grid is taken as a regular grid (uniform and rectangular). Care was taken to properly input the parameters so that the computational grid covers the whole of the bathymetric profile.

The SECTOR option was chosen for the spectral wave direction because it was a known fact that waves do not come with a spectral distribution over a full circle in a lab condition. However, trying to a trade-off between a real condition and a lab condition, a directional spreading of 30° was used, which should be 0° in the lab. Thus, the range of direction was 240° to 300° (as waves are coming at 270° w.r.t. North). To increase the computational accuracy, the number of meshes in θ-space was taken as 360 ($\Delta\theta = 1/6$). The range of discrete frequencies was 0.001 ([flow]) to 1 ([fhigh]) with [msc] = 100 (the grid resolution in σ-space $^{\Delta f}/_{f} = 0.0715$). The CIRCLE option was also tested as a condition to check its effect on the output. In this case, the parameters were so chosen that Δθ stayed 1/6.

Boundary Conditions

The default shape of the boundary condition in SWAN (and SWASH) is that of a JONSWAP Spectrum, with a peak enhancement factor γ of 3.3, and the directional width expressed in terms of power m itself in the distribution function $cos^m(\theta - \theta_{peak})$. This default spectral shape is used in the model.

Orientation

The lab flume is oriented in a West-East direction. The model replicates the same. In true sense, the direction does not matter in this study. The important point is that in SWAN the coast is perpendicular to the incoming waves. A visual representation is given in Figure A.1. The offshore side is in the West. The figure is generated by SWANOne, a graphical user interface (GUI) of SWAN, written on MATLAB. The script, written at the Delft University of Technology, uses full 2-D calculations. The SWAN model, however, is run in 1D mode.

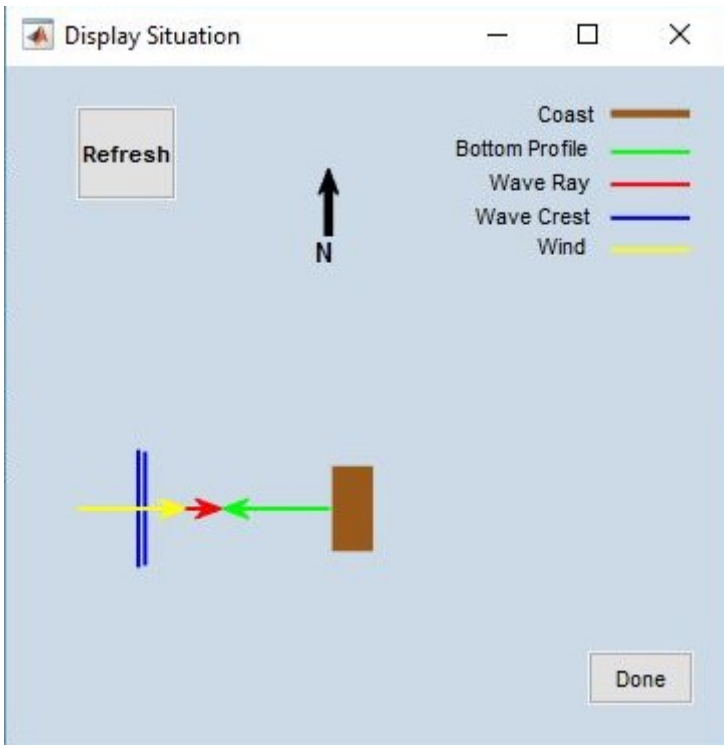

Figure A.1: Orientation of the flume (as generated by SWANOne)

Following this orientation, the input condition in SWAN in BOUndspec SIDE is W (for West). A constant spectrum is assumed.

Physics

Here, SWAN can be instructed to be run in first, second or third generation mode. The default of the 3rd generation with default parameters was used.

The physical conditions can be changed and used, as per the requirements. For example, a sensitivity analysis could be done to check how the parameters affect the results. For this lab condition, the nonlinear quadruplet wave interactions and diffractions were not considered. However, others, like white-capping, depth-induced wave breaking (can be specifically switched off, otherwise always considered), triad wave interactions, bottom friction, and setup are considered. Vegetation and mud are not considered, as they are not present in this situation. The default settings are applied.

Output

The output is requested in a tabular format. The output parameters and locations are decided as per the situation, even though SWAN calculates everything, requested or not. To get a spectral output (non-directional 1D (*.sp1 file*) and/or directional 2D (*.sp2 file*)) file, the locations desired can be specified and the output obtained. The quantity of output can be changed too, as per the expected values.

Lock-up

SWAN code must be finished with COMP only, if the stationary run is done, or the appropriate parameters for a non-stationary run added to the command. In this case, only COMP is used. COMP indicates SWAN to start the computations, either with stationary or non-stationary runs. Then the file is ended with STOP.

A.1.2. Regular Wave Input Script

```
$This is the regular wave run with a circle grid. In the sector case, in the CGRID line, $CIRCLE onwards is replaced with SECTOR 240 300 360 0.001 1 100
$------------------------------------------------------------
$         START-UP
$------------------------------------------------------------
$ (*) Start-up Commands
PROJECT 'Model A Run' '1'
SET NAUTICAL
SET LEVEL = 0
SET MAXERR = 2
SET DEPMIN = 0
MODE STAT ONED
$------------------------------------------------------------
$    MODEL DESCRIPTION
$------------------------------------------------------------
$ (*) Computational Grid
CGRID REG -14.7 0. 0. 37.7 0. 377 0 CIRCLE 36 0.001 1 100
$ (*) Input Fields
INPGRID BOT REG -14.7 0. 0. 377 0 0.1 0.
READINP BOT 1. 'marun1.bot' 1 0 FREE
$ (*) Boundary and Initial Conditions
BOUND SHAPE JONSWAP 3.3 PEAK DSPR POWER $This is default
BOU SIDE W CON PAR 0.07 2. 270. 2
$ (*) Physics
WCAP
OFF QUAD
TRIAD
BREAK
FRIC
SETUP
$------------------------------------------------------------
$    OUTPUT
$------------------------------------------------------------
CURVE 'curve' -14.7 0 377 23. 0
```

```
QUANTITY XP lexp=-14.7 hexp=23.0
Table 'curve' HEADER 'Model Analysis Run 1.1.tab' XP HSIGN DIR DSPR DEPTH
SETUP BOTLEV WATLEV
$-------------------------------------------------------
$    LOCK-UP
$-------------------------------------------------------
$ (*) Lock-up Input file
COMP
STOP
```

A.1.3. Spectrum Input for Bichromatic Wave

In this case, a bichromatic wave is used as an input. SWAN does not allow two wave parameters to be put simultaneously, as in, it does not consider two separate regular wave parameters as making up a bichromatic wave. For this, a spectrum is generated as explained in Appendix C. The conditions are same as in the regular wave case.

For the regular wave, put in a spectral format, the input file is also similar to the one below.

A.1.4. Spectral Input Script

```
$This is the bichromatic wave run with a circle grid. In the sector case, in the CGRID line,
$CIRCLE onwards is replaced with SECTOR 240 300 360 0.001 1 100
$-------------------------------------------------------
$         START-UP
$-------------------------------------------------------
$ (*) Start-up Commands
PROJECT 'Model A Run 1' '3'
SET NAUTICAL
SET LEVEL = 0
SET MAXERR = 2
SET DEPMIN = 0
MODE STAT ONED
$-------------------------------------------------------
$    MODEL DESCRIPTION
$-------------------------------------------------------
$ (*) Computational Grid
CGRID REG -14.7 0. 0. 37.7 0. 377 0 CIRCLE 36 0.001 1 100
$ (*) Input Fields
INPGRID BOT REG -14.7 0. 0. 377 0 0.1 0.
READINP BOT 1. 'marun1.bot' 1 0 FREE
$ (*) Boundary and Initial Conditions
BOUND SHAPE JONSWAP 3.3 PEAK DSPR POWER $This is default
BOU SIDE W CON FILE 'E_bichr.sp1' 1
$ (*) Physics
WCAP
OFF QUAD
TRIAD
BREAK
FRIC
```

```
SETUP
$------------------------------------------------------------
$    OUTPUT
$------------------------------------------------------------
CURVE 'curve' -14.7 0 377 23. 0
QUANTITY XP lexp=-14.7 hexp=23.0
Table 'curve' HEADER 'Model Analysis Run 1.3.tab' XP HSIGN DIR DSPR DEPTH
SETUP BOTLEV WATLEV
$------------------------------------------------------------
$    LOCK-UP
$------------------------------------------------------------
$ (*) Lock-up Input file
COMP
STOP
```

A.2. Model Validation

A.2.1. Surface Elevation and Bichromatic Wave Input

In this case, the input code did not change, because in this case, the input was only in the form of spectrum files for all cases: elevation, filtered elevation and bichromatic wave.

A.2.2. Input Code

```
$All model runs were done in the circle grid
$------------------------------------------------------------
$         START-UP
$------------------------------------------------------------
$ (*) Start-up Commands
PROJECT 'Validation Run 1' '1'
SET NAUTICAL
SET LEVEL = 0
SET MAXERR = 2
SET DEPMIN = 0
MODE STAT ONED
$------------------------------------------------------------
$    MODEL DESCRIPTION
$------------------------------------------------------------
$ (*) Computational Grid
CGRID REG -14.7 0. 0. 37.7 0. 377 0 CIRCLE 36 0.001 1 100
$ (*) Input Fields
INPGRID BOT REG -14.7 0. 0. 377 0 0.1 0.
READINP BOT 1. 'labrun1.bot' 1 0 FREE
$ (*) Boundary and Initial Conditions
BOUND SHAPE JONSWAP 3.3 PEAK DSPR POWER $This is default
BOU SIDE W CON FILE 'E_P1.sp1' 1 $This file varies per condition
$ (*) Physics
WCAP
OFF QUAD
```

```
TRIAD
BREAK
FRIC
SETUP
$------------------------------------------------------------
$    OUTPUT
$------------------------------------------------------------
CURVE 'curve' -14.7 0 377 23. 0
QUANTITY XP lexp=-14.7 hexp=23.0
Table 'curve' HEADER 'Validation Run 1.1.tab' XP HSIGN DIR DSPR DEPTH SETUP
BOTLEV WATLEV
$------------------------------------------------------------
$    LOCK-UP
$------------------------------------------------------------
$ (*) Lock-up Input file
COMP
STOP
```

B
SWASH SCRIPT

This appendix presents a brief overview of the SWASH script, otherwise known as the input code, as well as including a sample input file for each condition.

B.1. Benchmark Tests

B.1.1. Regular Wave

The SWASH code is very similar to the SWAN code. The similar commands are not explained in detail. The reader is requested to refer to Appendix A for this. The differences and exclusive commands are explained below.

Start-up

The Nautical Convention was used for the wave direction. The water level was set at 0. The maximum error level was set at 2. SWASH is run in 1D mode and in Non-Stationary Mode (time varying). Non-stationary is compulsory in SWASH.

Computational Grid

The computational grid is identical to SWAN case. However, in SWASH, the situation of spectral wave coverage (circle or sector) does not arise as SWASH is a time-domain model. A number for fluid layers can be stated (3D case), or if not mentioned, then it is a depth-averaged case (2D case). In this test run, it is considered depth-averaged to replicate the conditions as in SWAN.

Input Grid

The Input grid is the same as the SWAN model. Vegetation profile (as well as many other conditions) can also be read here into the model (same also in SWAN), but not used in this case.

Initial Conditions

No wind is used. To replicate the regular wave conditions, as in SWAN, the parameters were kept the same. In the case of 1D SWASH run, for a rectilinear grid, it does not require a wave direction, as it will always put the default, that is the incident wave angle normal to the boundary. The initial value of flow variables is taken as 0.

Boundary Conditions and Shape

The default JONSWAP spectrum is also used in SWASH, with the default parameters, with a weakly reflective condition. The orientation is the same, thus W (for West). A ramp function is applied to start-up the simulation smoothly. The smoothing period is taken as 5s.

Physics

For the SWASH run, bottom friction and breaking are taken into account. The default parameters are used. Others are not considered for this run. Breaking phenomenon and equation is different from what was employed in SWAN.

Numerics

Non-hydrostatic pressure is included in this run because the flow in case of short waves cannot be considered as hydrostatic. Discretization and time integration is considered explicitly with Courant numbers ranging from 0.1 to 0.5. This is recommended in case of presence of nonlinearities like wave-breaking.

Output

The output is requested in a tabular format. In the case of SWASH, the output can also be asked in a block format. This is helpful for data processing in MATLAB. The output variables, as required, can be obtained. The quantity of output can be changed too, like SWAN.

The duration of wave height must be provided, or SWASH will not run. This duration is for the part without the spin-up time.

Lock-up

SWASH code must finish with COMP. Unlike SWAN, since SWASH runs only in non-stationary mode, the parameters associated with COMP must be provided. The computational start and end time and the time step should be given. The spin-up time should be included in the computational time. Thus, the total computational time is the addition of the duration over which the significant wave height is calculated and the spin-up time. The file is ended with STOP.

B.1.2. Bichromatic Wave

In this case, a bichromatic wave condition is used as an input. SWASH does allow the input of two wave parameters in a Fourier series. The parameters required are the zero-frequency amplitude (here taken as 0 m) and the amplitudes (m), angular frequencies (rad/s), and phase (degrees) of the individual components.

B.1.3. Input Code

```
$This code is similar in both the cases. In the bichromatic wave case, in the BOUndcond
$line, the parts after CON is replaced with: FOURIER 0.  0.03 4.189 0.  0.04 2.513 0.
$------------------------------------------------------------
$         START-UP
$------------------------------------------------------------
$ (*) Start-up commands
PROJECT 'Model A Run 1' '1'
SET NAUTICAL
SET LEVEL = 0
SET MAXERR = 2
MODE DYN ONED
$------------------------------------------------------------
$    MODEL DESCRIPTION
$------------------------------------------------------------
```

```
$ (*) Computational Grid
CGRID REG -14.7 0. 0. 37.7 0. 377 0
$ (*) Input fields
INPGRID BOT REG -14.7 0. 0. 377 0 0.1 0.
READINP BOT 1. 'marun1.bot' 1 0 FREE
$ (*) Initial and Boundary Conditions
INIT ZERO
BOUND SHAPE JONSWAP 3.3 PEAK DSPR POWER $This is default
BOUndcond SIDE W CCW BTYPE WEAK SMOO 5 SEC CON REG 0.07 2.
$ (*) Physics
FRIC
BREAK
$ (*) Numerics
NONHYD
DISCRET UPW UMOM MOM $Good to use in case of wave breaking
TIMEI METH EXPL 0.1 0.5
$-----------------------------------------------------------
$    OUTPUT
$-----------------------------------------------------------
CURVE 'curve' -14.7 0 377 23. 0
$POINTS 'P_14.7m' -14.7 0
QUANTITY XP lexp=-14.7 hexp=23.0
QUANTITY HSIG DUR 60 MIN $The duration varies for the runtime tests
Table 'curve' HEADER 'Model Analysis Run 1.1.tab' XP HSIGN DEPTH SETUP BOTLEV
TABLE 'P_14.7m' 'Time series -14.7m MA Run 1.1.tab' TSEC WATLEV OUTPUT
000000.000 0.01 SEC
$The above table is for extracting a time series file for use in SWAN as a spectrum file.
$-----------------------------------------------------------
$    LOCK-UP
$-----------------------------------------------------------
$ (*) Lock-up Input file
COMP 000000.000 0.01 SEC 012000.000 $The end time varies for the runtime tests
STOP
```

B.2. Model Validation

B.2.1. Surface Elevation and Bichromatic Wave Input

In this case, the input code changes, per case, depending on the computation time, because SWASH is run for the same time as the laboratory run was done. Also, the boundary condition changes for either a time series input file or Fourier series parameters.

B.2.2. Input Code

```
$For Fourier Series condition, in the BOUndcond line, after CON, the Fourier parameters
$are used instead of a time series input file.
$-----------------------------------------------------------
$          START-UP
$-----------------------------------------------------------
```

```
$ (*) Start-up commands
PROJECT ‘Validation Run 1' '1'
SET NAUTICAL
SET LEVEL = 0
SET MAXERR = 2
MODE DYN ONED
$-----------------------------------------------------------
$    MODEL DESCRIPTION
$-----------------------------------------------------------
$ (*) Computational Grid
CGRID REG -14.7 0. 0. 37.7 0. 377 0
$ (*) Input fields
INPGRID BOT REG -14.7 0. 0. 377 0 0.1 0.
READINP BOT 1. 'labrun1.bot' 1 0 FREE
$ (*) Initial and Boundary Conditions
INIT ZERO
BOUND SHAPE JONSWAP 3.3 PEAK DSPR POWER $This is default
BOUndcond SIDE W CCW BTYPE WLEV SMOO 5 SEC CON SERIES 'etaP1.txt'
$ (*) Physics
FRIC
BREAK
$ (*) Numerics
NONHYD
DISCRET UPW UMOM MOM $Good to use in case of wave breaking
TIMEI METH EXPL 0.1 0.5
$-----------------------------------------------------------
$    OUTPUT
$-----------------------------------------------------------
CURVE 'curve' -14.7 0 377 23. 0
QUANTITY XP lexp=-14.7 hexp=23.0
QUANTITY HSIG SETUP DUR 46 MIN $The duration varies for different cases
Table 'curve' HEADER ‘Validation Run 1.1.tab' XP HSIGN SETUP BOTLEV WATLEV
$-----------------------------------------------------------
$    LOCK-UP
$-----------------------------------------------------------
$ (*) Lock-up Input file
COMP 000000.000 0.01 SEC 010548.790 $The end-time varies for different cases
STOP
```

C
INPUT CONVERSION

For SWAN input, especially the bichromatic wave input, it is necessary to put the input in the form of a spectrum. For that, SWASH was used to generate a surface elevation. Moreover, that time series was converted to a spectrum for using as input for SWAN. This appendix shows this conversion for the benchmark tests, but this procedure was also followed for the validation tests.

C.1. Regular Wave

The process is explained below by a conversion made for the regular wave in Chapter 3.

For a wave height of 0.07 m and period of 2 s, the following time series was obtained from SWASH (Figure C.1) at the offshore boundary (-14.7 m).

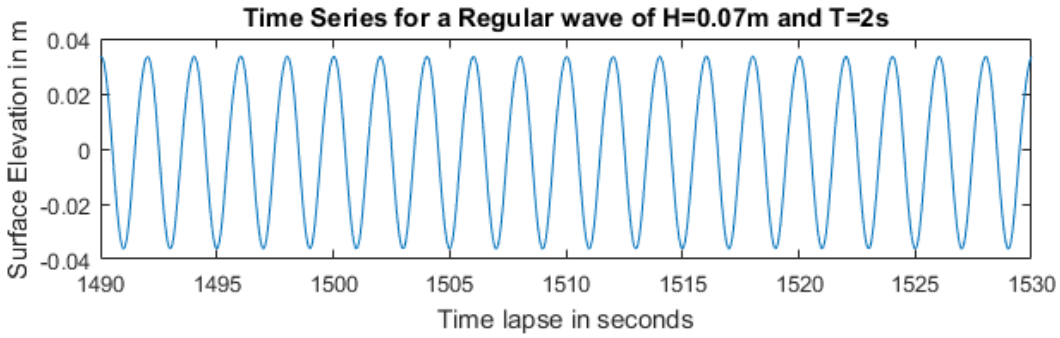

Figure C.1: Surface elevation for a regular wave, as generated by SWASH

This time series was converted to a variance density spectrum, and Figure C.2 shows the same. A spectral file in *.sp1* format was generated manually, for use in SWAN. The guidelines as in Appendix D of The SWAN User Manual was followed to generate such a file. It is important, in this step, to input the average direction and directional spreading carefully, for each energy density value. In this case, it was 270° and 30° respectively.

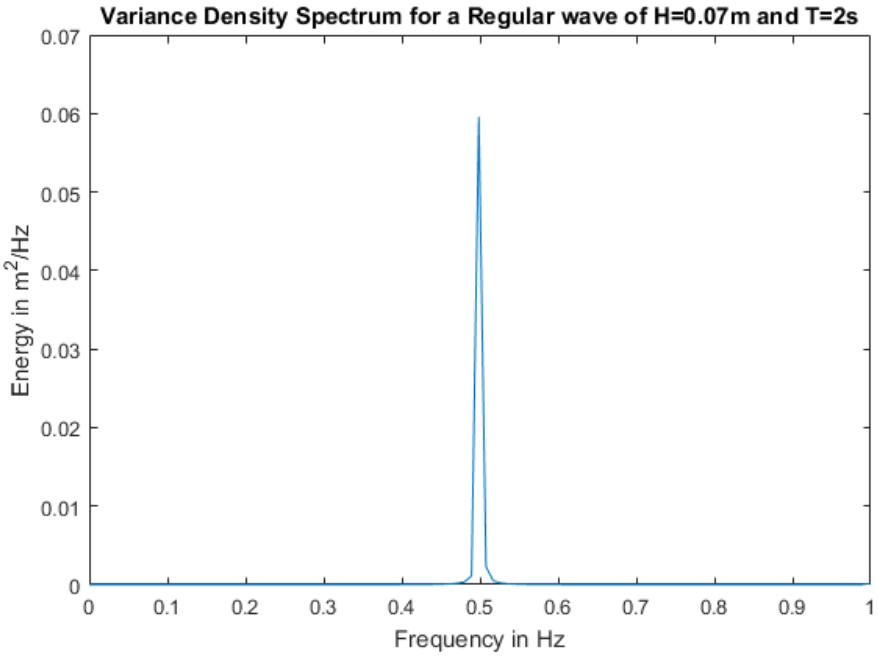

Figure C.2: Variance Density Spectrum for the regular wave time series

A Check of Input for SWASH

The input for the regular wave case was compared for either as single parameters or as a single component of a Fourier series.

This means that in the SWASH script terms, “REG 0.07 2.” was compared with “FOURIER 0. 0.035 3.142 0.” The output is presented in Figure C.3.

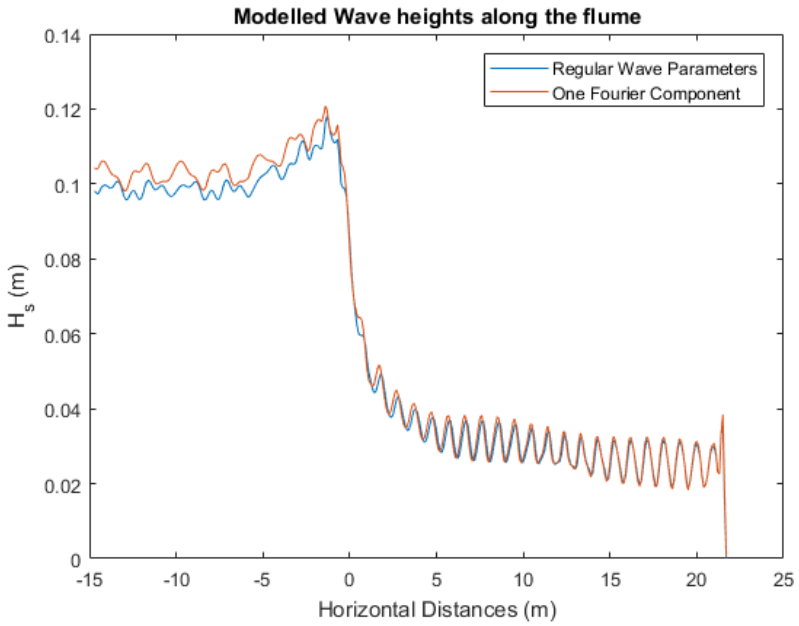

Figure C.3: SWASH-modelled wave heights along the flume

As seen, the difference in offshore is noticeable compared to the difference foreshore, which is negligible. However, for time constraints, the effects of different values offshore were not studied, and the model comparison in Chapter 3 was based on the regular wave parameter input.

C.2. Bichromatic Wave

A similar conversion was done for the bichromatic wave case. The time series and the variance density spectrum are shown in Figure C.4 and Figure C.5 respectively. Then a spectral input file for SWAN's use was manually generated.

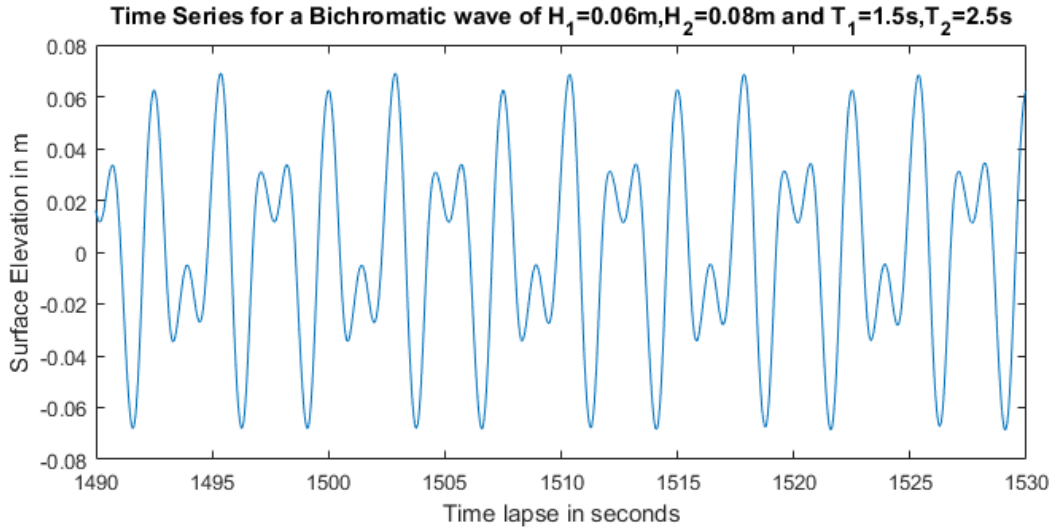

Figure C.4: Surface Elevation for a Bichromatic wave, as produced by SWASH

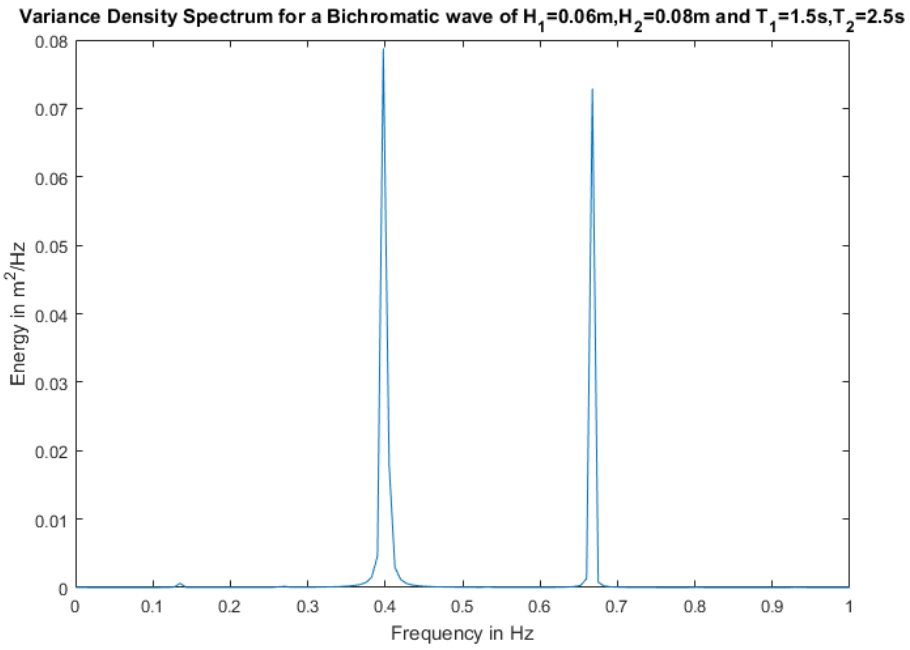

Figure C.5: Variance Density Spectrum for the bichromatic wave time series

D
Input Spectrum Sensitivity Analysis

SWASH model to get the input spectra for use by SWAN. This appendix touches upon what would be the variation of results, especially for the results in Chapter 3, without having to use SWASH to generate input spectra. The findings are presented below.

D.1. Regular Wave

Variance density spectrum for the case when it is created manually, i.e., without the help of SWASH time series and its subsequent conversion to VDS, is shown in Figure D.1. The reader is asked to compare this figure with Figure C.2. The shape is changed from being wide at the base to being just a spike in the signal at 0.5 Hz. However, the total energy amount is conserved while constructing the manual spectrum signal. The peak energy value is now 0.6 m^2/Hz contrasted with 0.06 m^2/Hz in the previous case.

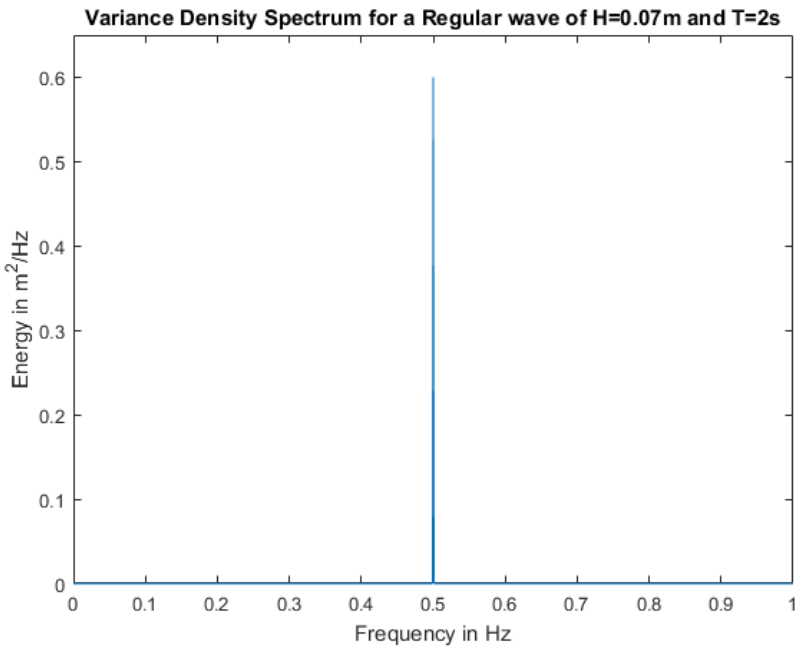

Figure D.1: Manually created VDS for the regular wave

The wave height values along the flume were obtained using SWAN for both the spectrum types and is presented in Figure D.2. As seen, the change in spectral input hardly affects the results, except having a slightly higher breaking height.

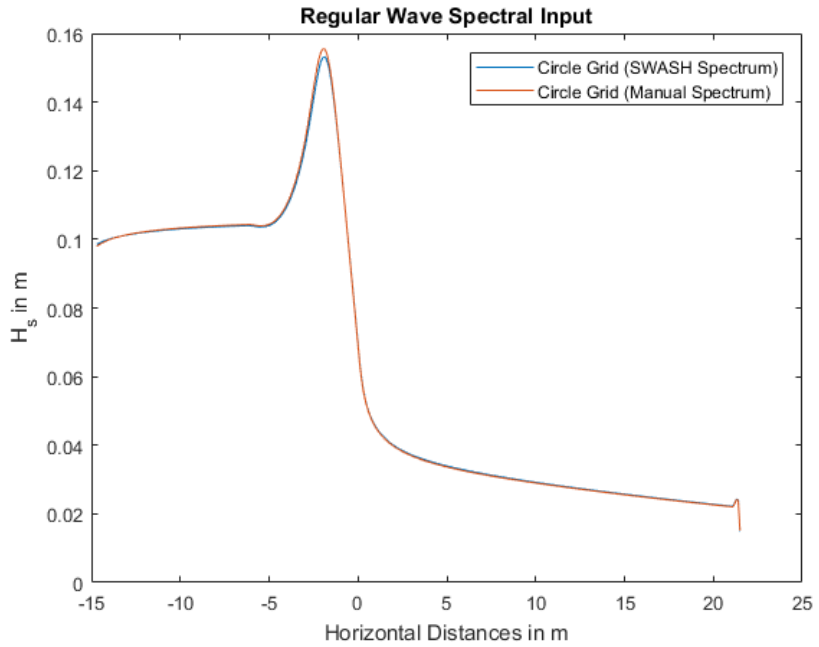

Figure D.2: SWAN Regular Wave case for two different types of spectral input

D.2. Bichromatic Wave

In a similar way, as above, a VDS was created manually for the bichromatic wave condition (still conserving the total energy content). It is presented below, in Figure D.3.

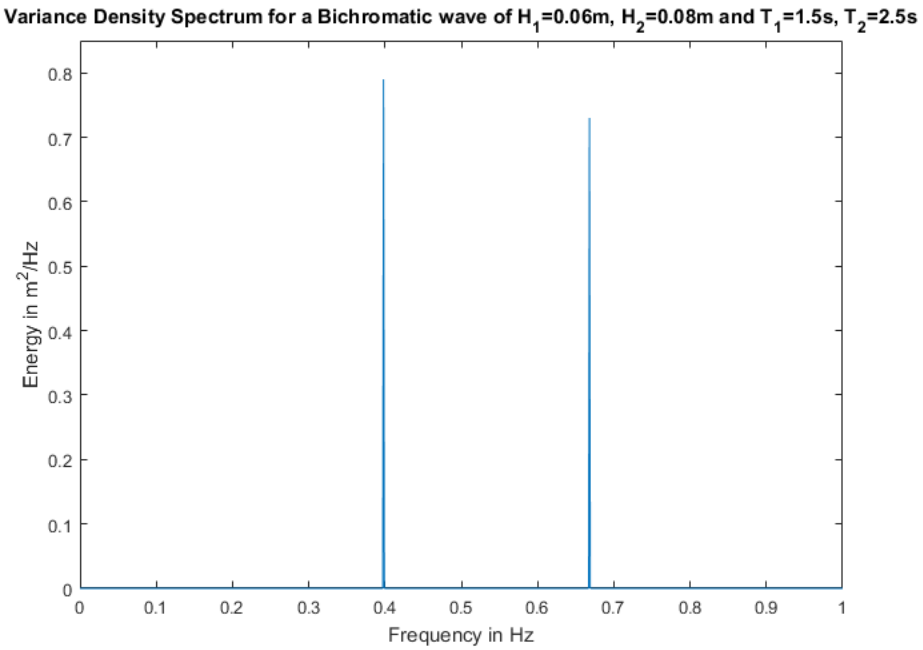

Figure D.3: Manually created VDS for the bichromatic wave

The corresponding wave heights (for spectra in Figure C.5 and Figure D.3) obtained from SWAN are presented in Figure D.4. As seen, the change in spectral input slightly

raises the offshore wave heights for the manual case, including the breaker height. After breaking, the difference is lost.

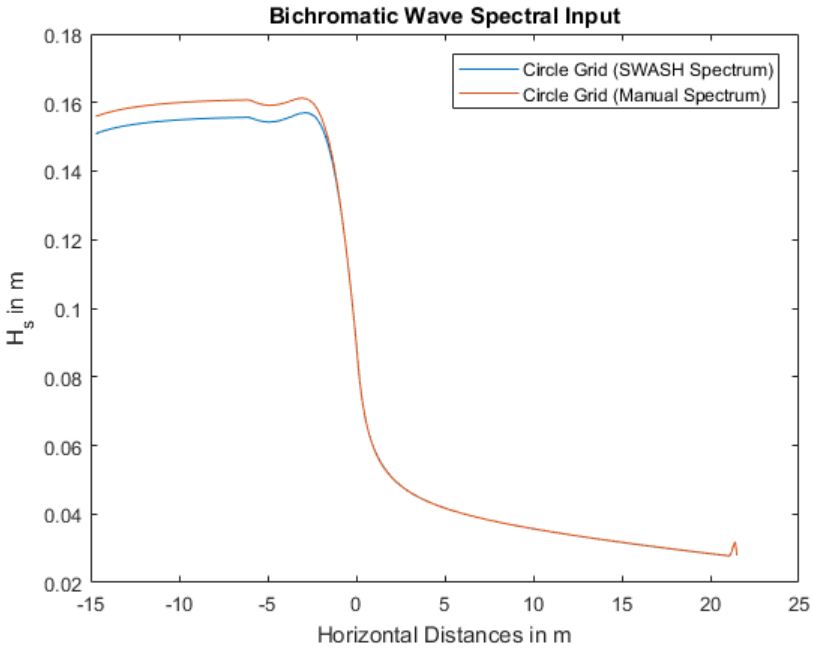

Figure D.4: SWAN Bichromatic Wave case for two different types of spectral input

After observing the results, it can be concluded that the spectra obtained from the SWASH-generated time series can be used with a satisfactory level of confidence. For the validation cases, if those are used, which they have been, the wave heights, especially the foreshore ones will not be much different for the manual spectra cases, provided that the total energy value is maintained. Due to time constraints, this could not be tested by the author.